

Micro-fabrication with Spark Assisted Chemical Engraving (SACE) Technology

Tohid Fatanat Didar

A Thesis

In

The Department

of

Mechanical and Industrial Engineering

**Presented in Partial Fulfillment of the Requirements
For the Degree of Master of Applied Science (Mechanical Engineering) at
Concordia University
Montreal, Quebec, Canada**

October 2008

© Tohid Fatanat Didar, 2008



Library and Archives
Canada

Published Heritage
Branch

395 Wellington Street
Ottawa ON K1A 0N4
Canada

Bibliothèque et
Archives Canada

Direction du
Patrimoine de l'édition

395, rue Wellington
Ottawa ON K1A 0N4
Canada

Your file *Votre référence*
ISBN: 978-0-494-63197-3
Our file *Notre référence*
ISBN: 978-0-494-63197-3

NOTICE:

The author has granted a non-exclusive license allowing Library and Archives Canada to reproduce, publish, archive, preserve, conserve, communicate to the public by telecommunication or on the Internet, loan, distribute and sell theses worldwide, for commercial or non-commercial purposes, in microform, paper, electronic and/or any other formats.

The author retains copyright ownership and moral rights in this thesis. Neither the thesis nor substantial extracts from it may be printed or otherwise reproduced without the author's permission.

AVIS:

L'auteur a accordé une licence non exclusive permettant à la Bibliothèque et Archives Canada de reproduire, publier, archiver, sauvegarder, conserver, transmettre au public par télécommunication ou par l'Internet, prêter, distribuer et vendre des thèses partout dans le monde, à des fins commerciales ou autres, sur support microforme, papier, électronique et/ou autres formats.

L'auteur conserve la propriété du droit d'auteur et des droits moraux qui protègent cette thèse. Ni la thèse ni des extraits substantiels de celle-ci ne doivent être imprimés ou autrement reproduits sans son autorisation.

In compliance with the Canadian Privacy Act some supporting forms may have been removed from this thesis.

While these forms may be included in the document page count, their removal does not represent any loss of content from the thesis.

Conformément à la loi canadienne sur la protection de la vie privée, quelques formulaires secondaires ont été enlevés de cette thèse.

Bien que ces formulaires aient inclus dans la pagination, il n'y aura aucun contenu manquant.


Canada

Abstract

Micro-fabrication with Spark Assisted Chemical Engraving (SACE) Technology

Tohid Fatanat Didar

Microfluidics and Lab-on-a-Chip devices have the potential to influence subject areas from chemical synthesis and biological analysis to optics and information technology. Micro fabrication is the means of turning the new designs and ideas in micro and nano technology into devices that benefit mankind. Among the materials used in microfluidic devices, glass has very interesting properties such as transparency, chemical resistance, bio-compatibility and low electrical conductivity. Conventional glass patterning can be performed via chemical or physical processes. Spark assisted chemical engraving (SACE) is an unconventional micro-machining technology based on electrochemical discharges used for micro-machining of non-conductive materials. SACE Glass 2D-micro-machining was characterized and parameters affecting the quality and geometry of the micro-channels were presented and the effect of each of the parameters assessed. Chemical contribution to the material removal mechanism is investigated. The results from the FT-IR analysis on the machined sample and Inductive Coupled Plasma Mass Spectrometry (ICP-MS) test showed that chemical etching at high local temperatures is the major phenomenon contributing to the machining process. Calculations of removed mass by analytical balance and geometrical methods, followed by the results from the nano-indentation test indicate that the hardness and density of the machined surface decrease during the machining process. Finally microfluidic components fully fabricated by SACE are presented.

Acknowledgments and Dedication

I remember the first semester, fall 2007, as I came to Concordia University everything was new, strange and seemed complicated to me. In the first discussions I had with Dr. Wuthrich about my research, he told me that I should first do some very simple 2D-micro-machining on glass substrates and it will be a new journal paper. Even right now I can clearly remember the way he was moving his hands to show me how simple it is to perform the 2D-micro-machining. Although it took me four months just to start the machining, but the motivation he gave to me as to how simple and easily I should be able to perform the experiments and write a paper through this work, helped me a lot. Whenever I faced a problem in the first months, I just thought that it is simple and I should be able to solve it. This helped me solve almost any problem I faced during my research. He also gave me the opportunity to openly discuss my ideas which sometimes seemed ridiculous. I hereby want to thank him for his motivation, guidance and great support of my ideas.

I would also like to thank Dr. Ali Dolatabadi for his great support, guidance and help. During my research I have benefitted from the help of many people: Dr. Mamoun Medraj, Dr. Paula Wood-Adams, Dr. Ion Stiharu, Mr. Heng Wang and Mr. Alian Tessier; I want to thank them all.

During the last four years, I have had the opportunity to love, live and be with someone who was not only my wife but also my best friend. She patiently listened to my ideas, problems and discussions and dedicated her time to me. Dear Soudeh, I know that this can never compensate what you did for me but I would like to dedicate my thesis to you. You have been and will always be in my heart.

Contribution of Authors

All papers presented in the thesis were entirely written by Tohid Fatanat Didar. All papers were co-authored with Prof. Rolf Wuthrich and Prof. Ali Dolatabadi (Department of Mechanical and Industrial Engineering, Concordia University), who acted as research advisors. All of the research presented in this dissertation was planned, performed, and critically analyzed by the author.

Chapter 1 is a thorough review of the field and introduction to the subject. Chapter 2 describes a novel procedure developed for 2D-micro-machining using SACE and its characterization. It includes computer programming and experimental work. Experiments, data collection and interpretation, computer programming and manuscript writing were performed by the author, with guidance from Prof. Rolf Wuthrich and Prof. Ali Dolatabadi. The work was published in *Journal of Micromechanics and Microengineering (JMM)* in 2008.

Chapter 3 elaborates the material removal mechanism in SACE micro-machining and includes different experiments about the material removal mechanism. This work was done under the supervision of Prof. Rolf Wuthrich and Prof. Ali Dolatabadi. The Inductive Coupled Plasma Mass Spectrometry (ICP-MS) tests were performed with help from Alian Tessier (Department of Chemistry, Concordia University). The results of this analysis will be submitted to the *Journal of Materials Chemistry* with R. Wuthrich and A. Dolatabadi as co-authors.

Chapter 4 investigates the changes in glass density machined with SACE. The experimental design and implementation, material characterization and manuscript writing were performed by the author, with guidance from Prof. Rolf Wuthrich and Prof.

Ali Dolatabadi. The nano-indentation tests were performed with help from Mr. Heng Wang. This work was published in *Materials Letters* in 2008. Chapter 5 is the conclusion of the thesis including applications developed and ideas for the future work.

Table of Contents

List of Figures.....	x
List of Tables.....	xi
Chapter1: Introduction.....	1
1.1. History of electrochemical discharges.....	2
1.2. Spark Assisted Chemical Engraving (SACE).....	3
1.2.1. General principle.....	3
1.2.2. SACE micro-machining set up.....	4
1.3. Glass micro-machining.....	6
1.3.1. Micro-hole drilling.....	6
1.3.2. 2D-micro- machining.....	8
1.4. Material removal mechanism.....	9
1.5. Thesis objective and overview.....	9
Chapter 2: Glass 2D-Micro-Machining.....	11
2.1. 2D-micro-machining procedure.....	12
2.2. Results and discussion.....	14
2.2.1. Quality of machined micro-channels.....	14
2.2.2. Geometry of machined micro-channels.....	18
2.3. Proposal of a model for micro-channels quality as function of voltage and speed.....	22
2.4. Comparison of experimental data with theory.....	26
2.4.1. Heat transfer model and experimental results.....	26

2.4.2. Chemical etching model and experimental results.....	28
2.5. Conclusion	31
Chapter 3: Material Removal Mechanism.....	33
3.1. Chemical etching in SACE micro-machining.....	34
3.2. Parameters affecting the material removal mechanism.....	35
3.3. Experimental Procedure.....	36
3.4. Results and discussions.....	38
3.4.1. Depth profile variation with electrolyte concentration	38
3.4.2. FT-IR analysis of the machined samples	41
3.4.3. Material removal assessment	42
3.4.4. ICP-MS test for silicone concentration inside machined samples	43
3.4.5. Discharge regime and exposed energy in different electrolyte concentrations.....	44
3.4.6. Different micro-channel contours using different electrolyte concentrations.....	46
3.5. Conclusion	48
Chapter 4: Glass Surface Modification by Electrochemical Discharges.....	49
4.1. Experimental procedure	50
4.2. Results and discussions.....	52
4.3. Etching machined samples with HF.....	55
4.4. Conclusion	56
Chapter 5: Conclusions, Original Contributions to knowledge and Future Prospective.....	57

5.1. Simultaneous micro-hole drilling and micro-channel machining	58
5.2. Simple techniques to enhance surface quality	59
5.3. Proposal of a new microfluidic device for statistical studies in bio applications.....	60
5.4. Fabrication of micro-mixers based on surface roughness.....	61
5.5. Conclusions and original contributions to knowkedge	63
5.6. Ideas for future work.....	65
References.....	66
Appendix: Examples of computer codes developed for micro-machining.....	70

List of Figures

Figure 1-1. Schematic presentation of electrochemical cell	3
Figure 1-2. a) Schematic representation of the experimental set-up, b) machining set-up.....	5
Figure 1-3. Schematic representation for gravity-feed micro-hole drilling	6
Figure 1-4. Characterization guide for for micro-hole drilling	7
Figure 1-5. Micro-holes drilled with 28-30V and 200 microns depth	7
Figure 2-1. Schematic representation for 2D-micro-machining with constant velocity	13
Figure 2-2. Channel contours.....	17
Figure 2-3. Quality of the surface of machined micro-channels.....	18
Figure 2-4. Micro-channel depth as a function of machining time.....	19
Figure 2-5. Micro-channel depth profile.....	20
Figure 2-6. Initial micro-channel depth in 28V and 30V as a function of tool speed.....	21
Figure 2-7. Micro-channel depth profile at different tool distances from glass surface	22
Figure 2-8. Characterization diagram for micro-channels machined by SACE	23
Figure 2-9. Schematic representation for accumulation of removed material on micro-channel surface for higher voltages at low speeds.	25
Figure 2-10. Comparison between experimental data and proposed theoretical model for speed limit needed to have micro-channel formation	28
Figure 2-11- Chemical etching in different temperatures according	29
Figure 2-12-a) Increase in rate of micro-channel depth as a function of tool speed in different voltages b) Predicted local chemical etching temperature for different tool speeds.....	30
Figure 3-1-Comparison of machining with an active cathode and anode.....	35
Figure 3-2. Initial depth machined with different electrolyte concentrations.....	40
Figure 3-3. Increasing trend in depth of micro-channels with electrolyte concentration	40
Figure 3-4. FT-IR analysis of the machined sample.....	41
Figure 3-5. Material removed from the glass surface during 2D-micro-machining	43
Figure 3-6. Critical voltage for different electrolyte concentrations.....	45

Figure 4-1. Schematic representation of the experimental procedure.....	51
Figure 4-2. Material removed based on measuring samples weight before and after machining and based on calculated volumetric removed mass	53
Figure 4-3. Force-Displacement graphs of nano-indentation test before and after machining.....	54
Figure 5-1. Micro-channel with two all-through holes as inlet and outlet.....	59
Figure 5-2. 3D view of the design drawing for the simple device	59
Figure 5-3. 3D-design of a microfluidic device for statistical study in bio applications	61
Figure 5-4. Micro-channel machined with 10 %wt NaOH electrolyte	62
Figure 5-5. Y shape microfluidic device with inlet and outlet wells fabricated by SACE for mixing applications.....	62

List of Tables

Table 3-1. Results of ICP-MS test on 40 wt% electrolyte.....	44
Table 1-1. Percent deviations of the removed mass calculations by two different techniques	53

1. Introduction

The manipulation of fluids in channels with dimensions of tens of micrometers, microfluidics, has emerged as a distinct new field. Microfluidics and Lab-on-a-Chip devices have the potential to influence subject areas from chemical synthesis and biological analysis to optics and information technology.[1]

Glass, silicon and some polymers are considered the most used materials for microfluidic devices. Among these, glass has very interesting properties such as transparency, chemical resistance, bio-compatibility and low electrical conductivity. Various technologies are available for patterning micro-holes and micro-channels on glass. [1]

Conventional micro-fabrication can be performed via chemical or physical processes. Lithography is used as the most famous chemical process which utilizes chemical etching. These methods of fabrication are, however, often very time-consuming and expensive as they involve several steps such as substrate cleaning, lithographic patterning, wet-etching and bonding. Besides, achieving high aspect ratio structures with chemical etching, such as connecting holes, is challenging to obtain.

On the flip side, other established glass micro-machining technologies are physical, such as laser machining, abrasive jet machining, ultrasonic machining, water jet machining and diamond cutting. Compared to the clean room technologies, these methods are in general single processes and often hampered by the difficulty in obtaining a good surface quality leading to structural damages like micro-cracks. Among physical processes, laser micro-machining is the most developed which performs micro-machining with local heating of the surface [2]. Although expensive equipment used in laser machining results in high production costs [2].

Spark assisted Chemical Engraving (SACE) is an unconventional and novel technology which can be used for micro fabrication [3]. Ability of this technology to combine local heating and local chemical etching has enabled it to take the advantage of both chemical and physical processes for fabrication. The most notable property of SACE is its ability to localize these processes which enables its application to micro fabrication and reduces prototype production costs significantly. SACE not only eliminates the need for clean-room environment, but also provides the possibility of simultaneous fabrication of a set of micro-holes and micro-channels only by moving the machining tool. The whole process does not take more than 4 hours for a complex device [4, 5] and high aspect-ratio structures can be obtained. Typical dimensions of machined structures reach from around 100 μm up to a few centimeters.

1.1. History of electrochemical discharges

Electrochemical discharges were first used by physicians as a source of light spectra in the middle of the 19th century. This physical phenomenon was rediscovered in the beginning of the 20th century by electrical engineers as nonlinear electrical components and again in the middle of last century by chemists as a source of non faradic electrochemical reactions. Its use in micro machining dates back to the second half of the 20th century by H. Kurafuji and K. Suda [6]. So far the latest development has been the synthesis of nanoparticles [7]. Each of these applications is actually hosted in different fields of science and engineering. This explains why at the beginning of each of these applications, the electrochemical discharge phenomenon was rediscovered and only later related to earlier observations reported in other fields.

1.2. Spark Assisted Chemical Engraving (SACE)

1.2.1. General principle

Electrochemical Discharge Machining (ECDM) or Spark Assisted Chemical Engraving (SACE) was first introduced by Kurafuji *et al.* [6]. While SACE has been used for machining of different materials such as ceramics and silicon [8, 9], glass has been subject to considerable attention because of its excellent properties for microfluidic and Lab-on-a-Chip devices.

The machining takes place in an electro-chemical cell where the cathode is used as the machining tool and the anode as a counter-electrode [10]. When a voltage higher than a critical value, called critical voltage, is applied, bubbles grow so dense on the tool electrode that they coalesce into a gas film; this has been identified as one of the key parameters for machining repeatability [3, 11]. Electrical discharges take place between the tool electrode and the electrolyte (figure 1-1). When the tool electrode is brought in close vicinity (less than $25\mu\text{m}$ for glass [3]) of the substrate, machining takes place.

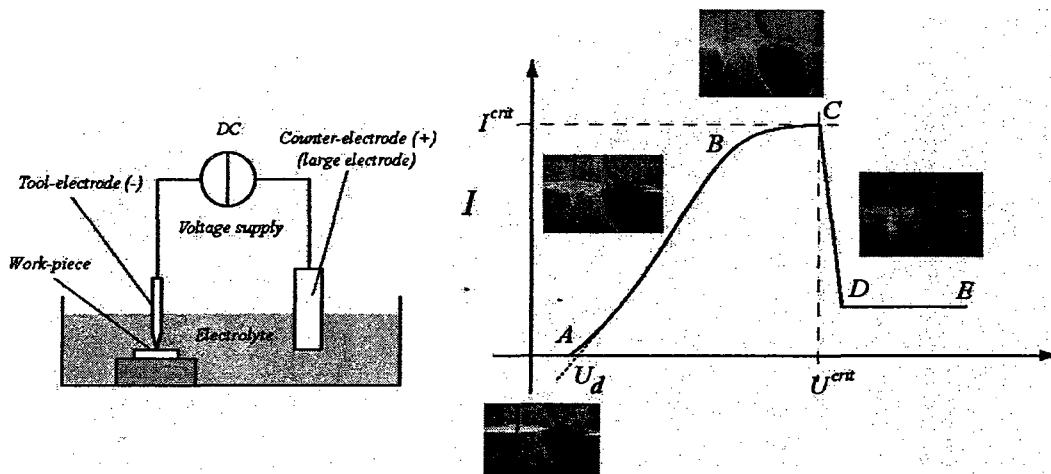


Figure 1-1. Schematic presentation of electrochemical cell and current-voltage characteristics

The value of the critical voltage U_{crit} is function of the inter-electrode resistance and is determined by the condition that the current density on the tool-electrode is at least 1 A/mm^2 . Typical values are around 25V. Detailed descriptions of the fundamentals of the gas film formation are reported in the literature [3, 11, 12].

1.2.2. SACE micro-machining set up

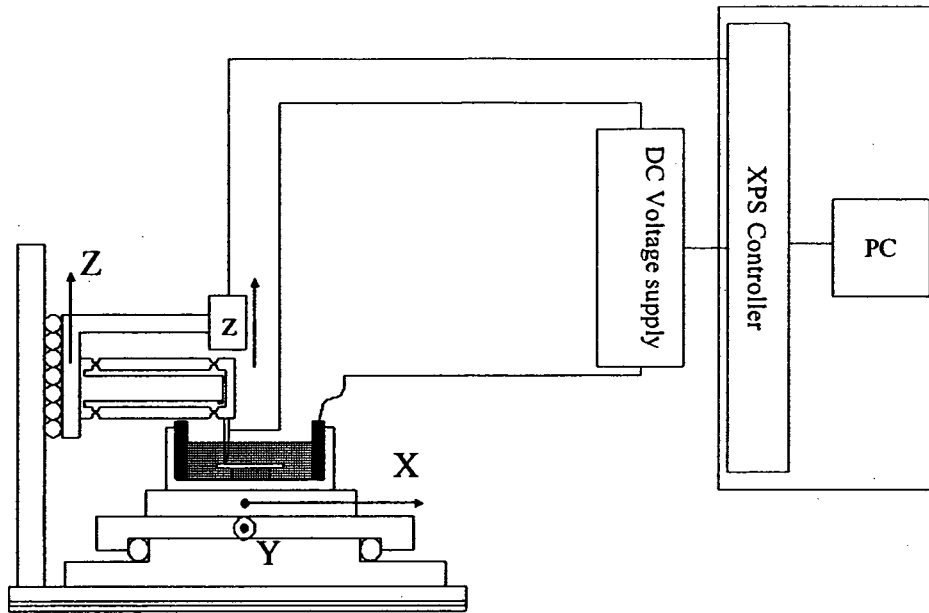
The experimental set-up for SACE micro-machining has schematically been shown in figure 1-2a. The main parts of the set-up are the following:

- Electrochemical cell
- Power supply
- XYZ-stages
- Programmable controller
- Tool electrodes of different shapes and material

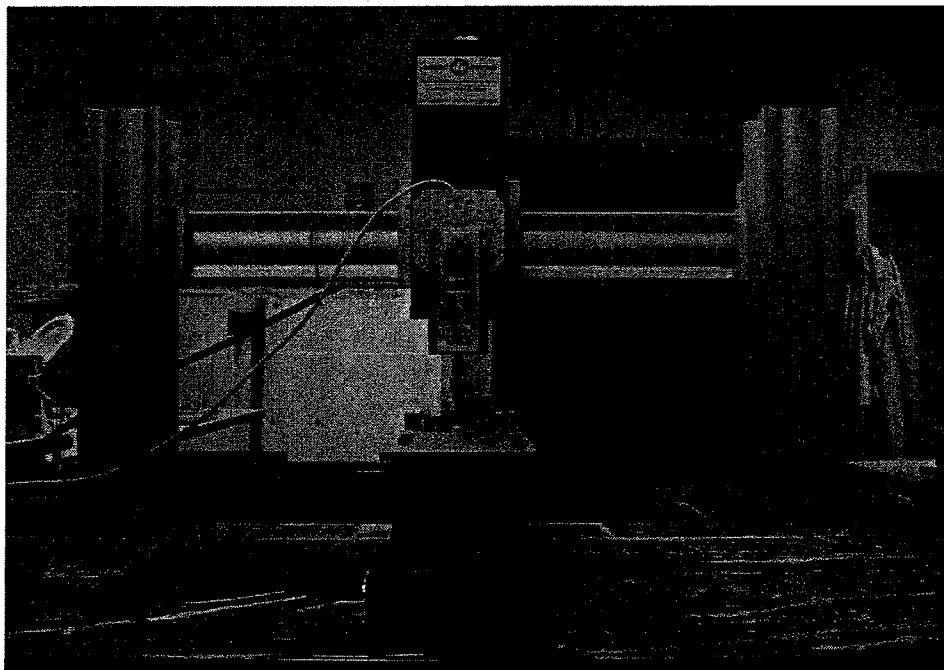
The setup shown in figure 1-2b has the advantage of 3D motion, i.e. the drilling head can move simultaneously along the three axes to follow a 3D trajectory. The processing cell is mounted on an XY stage with the work-piece and on a Z stage the machining head with the fixed tool electrode. XYZ stages are from Newport® which are controlled using an XPS motion controller from the same company. The machining head consists of a homemade flexible structure which allows detecting the glass surface for 2D-machining.

As a counter electrode, a large cylindrical ring (same diameter as the processing cell) in stainless-steel is used. The work-pieces are standard glass sample holders for optical microscopes with a thickness of 1 mm (Menzel-Gläsner, a soda-lime glass). The

processing cell is cylindrical with a diameter of 11 cm. The power source used in the experiments is a commercial power source Lambda Zup (60V-3.5A).



(a)



(b)

Figure 1-2. a) Schematic representation of the experimental set-up, b) machining set-up

1.3. Glass micro-machining

1.3.1. Micro-hole drilling

Micro-hole drilling in glass is an important task to realize connections to, or between, layers for micro-fluidic devices. SACE is particularly suited for such tasks because of the possibility to machine a wide range of hole diameters and forms with high aspect-ratio [3, 5, 13]. The most efficient and simple way of micro-hole drilling with SACE is to use the so called gravity-feed drilling [13]. The tool-electrode moves down inside the work-piece by its own weight or alternatively by a constant force pushing on it. Even when no extra control for the drilling process is used, the micro-hole depth is easily controllable with a precision of a few microns [5]. Figure 1-3 shows the steps for gravity-feed drilling.

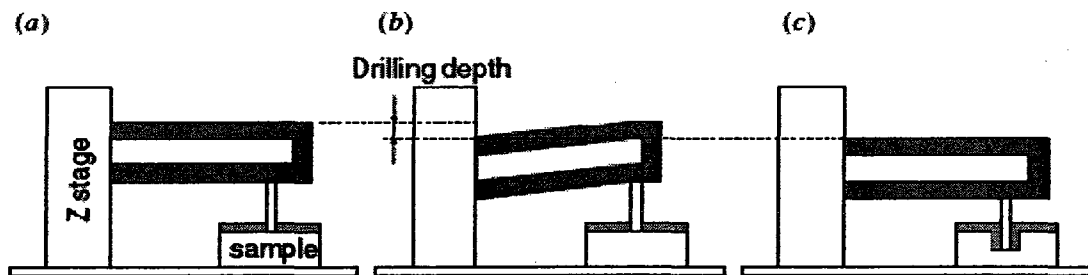


Figure 1-3. Schematic representation of different steps for gravity-feed micro-hole drilling a) glass surface is detected b) machining head is moved down the desired micro-hole depth and the voltage is switched on c) desired depth is reached and the voltage is switched off [13]

Using an additional sensor (e.g. optical sensor) the progress of the drilling can be monitored during the process. The analysis of the drilling reveals that after a few hundred

microns, the process becomes limited by the ability of the electrolyte to reach the tool-electrode tip resulting in an almost constant drilling speed of about 10-20 $\mu\text{m/s}$ and an increase of the micro-hole diameter [5].

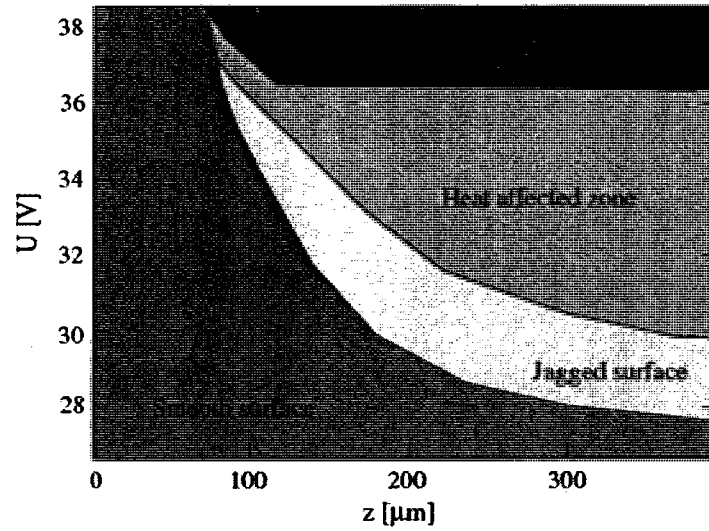


Figure 1-4. Characterization guide for choosing proper voltage as a function of desired depth for micro-hole drilling [5]

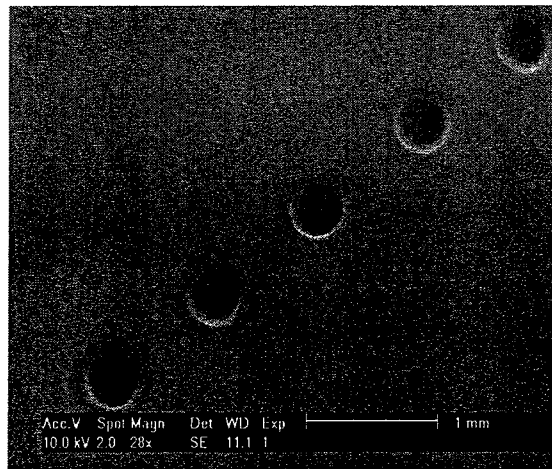


Figure 1-5. Micro-holes drilled with 28-30V and 200 microns depth [13]

Figure 1-4 helps in selecting the right voltage as a function of the desired precision, surface quality and drilling depth. If needed, some additional vibration can be added to the tool motion to reduce machining time or voltage pulses can be used to reduce the heat affected zone around the micro-holes [14]. Figure 1-5 shows micro-holes drilled applying parameters on the blue zone (smooth surface) shown in figure 1-4.

1.3.2. 2D-micro-machining

It is possible to perform 2D and 3D machining by moving the tool over the working piece [15-17]. This was reported first by Langen *et al.* [18]. Later Wüthrich *et al.* [18-20] reported micro-channels of 100 μ m width and a few millimetres long. Recently the effect of tool rotation and pulse voltage [21] and electrolyte composition [22] on the performance of 2-D-micro-machining have been reported. However none of these studies were designed to improve understanding of the key mechanisms controlling the quality and geometry of micro-channels.

The quality and geometrical specifications of machined micro-channels has so far never been characterized systematically. As micro-channels play a vital role in MEMS, micro-fluidic or Lab-on-a-Chip devices, the quality of machined channels and depth of the channels must be well controlled.

Obtaining an acceptable quality for micro-channels with SACE is more challenging than micro-holes. The most appropriate method for machining is to keep the tool-electrode a few microns above the glass surface (typically less than 25 μ m) and move it at a constant speed. As it is impossible to align the glass surface to be completely horizontal, there will be a difference in the height of the start and end points of the micro-channel. The

horizontal motion of the tool will change its distance from the glass surface and there will even be a possibility of contact between glass surface and the tool. A systematic method for 2D-micro-machining resulting in characterization and modeling is introduced in chapter 2.

1.4. Material removal mechanism

As discussed before, machining with electrochemical discharges was introduced in the pioneering work of H. Kurafuji and K. Suda [6] on glass micro-drilling. Since this subject has been studied by several researchers, however there is a significant lack of knowledge when it comes to the mechanism of material removal in SACE. Several processes are thought to contribute to material removal [23, 24]:

- Melting and vaporization due to electrochemical discharges
- High temperature chemical etching
- Differential expansion of constituents and weathering
- Random thermal stresses and micro-cracking and sapling
- Mechanical shock due to expanding gases and electrolyte movement

Different groups attributed the material removal mostly to a combination of “thermal melting due to local heating by the electrochemical discharges and some chemical effects” [3, 25-27].

1.5. Thesis objectives and overview

The main objective of this thesis is to systematically characterize the novel SACE technique so that it can be confidently used for fabrication of micro fluidic devices. In order to achieve this goal, the following requirements should be fulfilled:

1- Systematic characterization of 2D-micro-machining: Micro-holes and micro-channels are the main parts of any microfluidic device. As mentioned before, micro-hole drilling by SACE has been developed and characterized but there was a lack of knowledge for systematic performing and characterization of 2D-micro-machining. 2D-micro-machining will be discussed in chapter 2.

2- Mechanism of material removal: Understanding the mechanism of material removal can help in developing better experimental set-ups and control strategies for micro-fabrication. Material removal mechanism and chemical effects during machining process will be discussed in chapter 3.

3- Changes in machined samples properties: Properties of machined glass substrates such as hardness and local density are important parameters not only for the future applications of the machined substrates but also for better understanding of the material removal mechanism. Changes in hardness and density of machined glass samples, confirmed by performing nano-indentation test on the machined micro-channels surface, is discussed in chapter 4.

Recently, micro-holes machined with SACE have been used for different applications. The micro-channels in the recent applications have been fabricated via other methods *e.g.* laser machining or photolithography. In Chapter 5, a microfluidic device comprised of micro-holes and micro-channels machined with SACE is introduced for the first time. In addition to the conclusion of the thesis, some original ideas for future studies about the applications of SACE for fabrication of microfluidic and Lab-on-a-Chip devices are also proposed in chapter 5.

2. Glass 2D-Micro-Machining

This chapter elaborates characterization of SACE 2D-micro-machining with constant speed and proposes a practical model for achieving desired micro-channel contours. Besides, Parameters affecting the quality and geometry of the micro-channels machined by SACE technology with constant velocity is presented and the effect of each parameter is assessed. Results from variety of experiments provide a quantitative description of achievable geometrical tolerances and micro-channel quality using SACE constant velocity machining. The study focuses on the characterization of achievable geometrical tolerances as a function of the machining voltage and tool speed. The impact of chemical etching in SACE-2D-micro-machining is quantified. The machined micro-channels are characterized and a phenomenological model for SACE constant velocity 2D-machining is proposed and was shown to have firm theoretical bases.

This chapter is based on the following publication:

Fatanat Didar T., A. Dolatabadi, R. Wuthrich , *Characterization and Modeling of 2D Glass Micromachining by Spark Assisted Chemical Engraving (SACE) with Constant Velocity, Journal of Micromechanics and Microengineering* 18(2008) 065016.
doi: 10.1088/0960-1317/18/6/065016.

2.1. 2D-micro-machining procedure

In the first step, the machining head is positioned on the XY stage at the desired position. The Z stage is slowly moved down (at $200\mu\text{m/s}$) until the machining head touches the glass surface. This point will be the end point of the micro-channel. The Z stage speed is chosen slow enough to get repeatability in the surface position detection smaller than $5\mu\text{m}$. When the glass surface is detected, the Z stage is moved up and then the X stage moves to obtain the desired channel length (15mm). Then, the Z stage is moved down, according to the same procedure as the first point, to detect the second point of the channel. The two detected points will define a line in the XZ plane. Using these two points, the equation of a line is formed: the ideal trajectory. The ideal trajectory can only be followed for a surface which is completely smooth; the notion of a smooth surface is meaningless at micro scale and any real surface exhibits defects at this scale. The glass samples used in the experiments are guaranteed by the manufacturer to have surface defects smaller than 1 micron. Therefore surface irregularities can be neglected and the ideal trajectory has to be modified only to take the machine error into account to avoid the machining tip touching the surface. This error is attributed to the system which is used for glass surface detection and is measured to be approximately 3 microns. The primary line is then shifted along the Z axis in an amount equal to this error plus the desired tool distance from glass surface. The shifted line, which is called the “practical trajectory”, is the trajectory followed by the machining tip (figure 2-1).

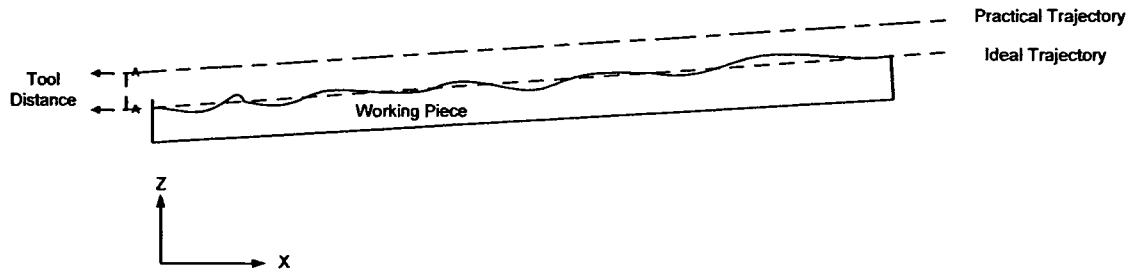


Figure 2-1. Schematic representation for 2D-micro-machining with constant velocity

After finding the equation of the practical trajectory, the machine tip is moved to the first point of the practical trajectory, the voltage is switched on and the tip is moved along this trajectory. The magnitude of the velocity vector in the XZ plane is kept at a pre-specified constant value. When the tool reaches the last point of the practical trajectory, voltage is switched off and the process for 2D-machining is finished.

The next step is to measure the depth of the channel. The procedure used to measure the machined micro-channel depth is as follows: 10 points are chosen along the machined micro-channel, the machining tip is kept at a safe distance from the surface (about 3mm) and moves through these points consecutively, on each point the tip moves along the Z axes until it touches the channel surface at which point the coordinate of the point is saved. Comparing this coordinate with the analogous point on the ideal trajectory, the depth of the micro-channel at that point is obtained. These points were chosen to be in the middle of the micro-channel (with 2mm distance from two ends) to avoid boundary effects. Since the tip itself has a finite thickness, the measured values have to be interpreted with care. These measured depth values were verified and confirmed using an

optical microscope. To automate the procedures explained above, computer programs were developed using the TCL scripting language.

2.2. Results and discussion

Several parameters affect the quality and geometry of micro-channels fabricated by SACE technology with constant velocity, the most important of which are tool speed, applied voltage, tool distance from glass surface, thickness of electrolyte layer above glass surface and tool travel length. It is very difficult to control the thickness of the electrolyte layer above the glass surface; therefore this parameter was not used as a variable and in all the experiments the same amount of electrolyte was used. Various experiments were performed to find out the effect of the other parameters on machined micro-channels. All the experiments were done with a tool distance of about 5 microns from the glass surface. Only in the experiments which were performed to study the effect of the tool distance from the glass surface, this distance was varied. The electrolyte used for 2D-micro-machining, was 30%wt NaOH. Its mean temperature was the ambient temperature before starting the machining in all experiments. The tool electrodes were cylindrical electrodes of 0.5 mm in diameter 316 L stainless steel. The shape of the electrodes was inspected prior to the machining with an optical microscope and if necessary corrected using emery paper. In the following sections the results will be discussed including the quality of machined channel and their geometrical characteristics.

2.2.1. Quality of machined micro-channels

As the tool is moved above the glass surface for 2D-micro-machining, the first question is to find out the upper limit of velocity in which a micro-channel is formed. Whether a

micro-channel is formed depends not only on the tool speed but also on the applied voltage and tool distance from the working piece. In some speeds it is not possible to have any micro-channel formation. This limit varies for different voltages, for example in 28V it is not possible to have any acceptable channel shape for speeds $>40\mu\text{m/s}$ and for 30V this limit is $>50\mu\text{m/s}$.

On the other hand, applying high voltages (more than 32V) at low speeds results in unsmooth channel surface with significant depth variation along the channel surface. The quality of the micro-channels deteriorates as the tool speed is decreased. This can be attributed to poor material removal rate and accumulation of removed material inside the previous machined micro-channel surfaces.

In other cases it is possible to have micro-channels with edges and surfaces of acceptable quality. Concerning the above mentioned points, following contours can be distinguished as a function of machining voltage and tool speed:

1. Well-defined linear channel edges and smooth channel surface

This type of counters is a characteristic for low voltages with appropriate constant velocity. This format can be found in 28V with tool speed ranging from $5\mu\text{m/s}$ to $10\mu\text{m/s}$ and 30V with tool speed ranging from $15\mu\text{m/s}$ to $30\mu\text{m/s}$ (Figure2-2a and figure2-3a).

2. Jagged out line contours with smooth channel surface

This contour is observed for lower voltages (less than 32V) with speeds lower than in the previous contour type. In this counter the micro-channel edges are jagged out but the

channel surface is still flat and smooth, as for example in 30V when the speed is reduced to lower than $15\mu\text{m/s}$ (Figure2-2b and figure2-3b).

3 .Heat affected edges with smooth channel surface

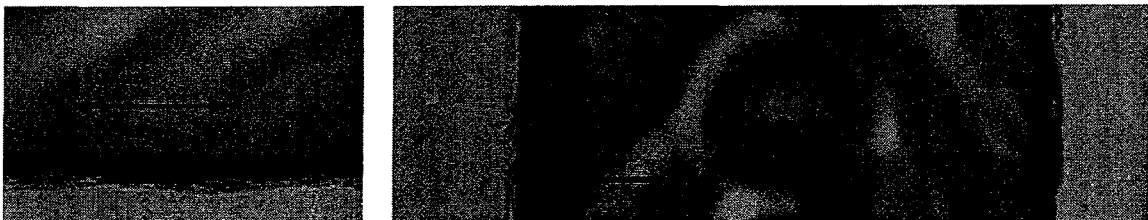
This counter belongs to higher voltages (more than 32V) with speeds high enough to remove the melted material. In these conditions, the micro-channels will exhibit smooth channel surface but the channel boundaries are not well defined due to the effect of heat generation (Figure2-3c and figure2-4c).

4 .Heat affected edges with unsmooth channel surface and thermal cracks

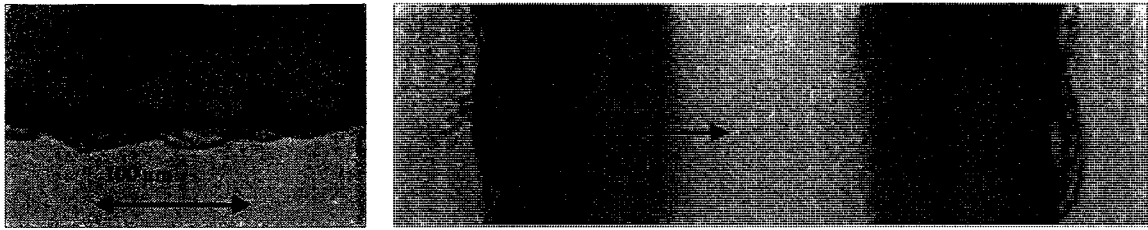
When the speed is low at high voltages (32V with speed less than $30\mu\text{m/s}$ and 35V with speed less than $40\mu\text{m/s}$) the edges are unclear and heat affected and the surface is not flat and smooth with thermal cracks (figure 2-2d and figure2-3d).

5. Deteriorated micro-channels (discretized boundaries with unsmooth surface and varying depth)

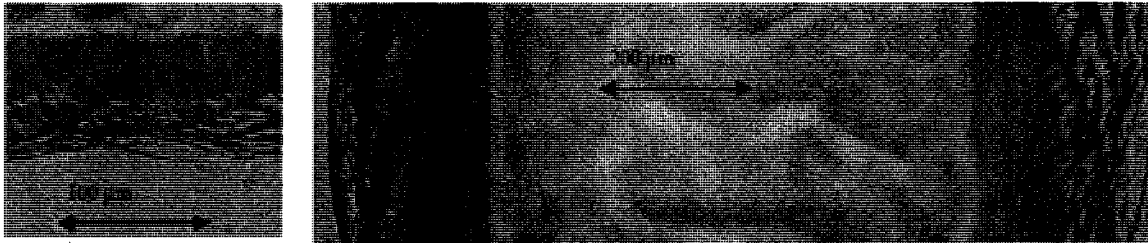
As the tool speed is increased, the channel will be discretized and the inside surface will be very rough. For example in 28V increasing the speeds above $40\mu\text{m/s}$ will result in deteriorated micro-channels. (figure 2-2e)



(a) Well-defined linear channel edges and smooth channel surface



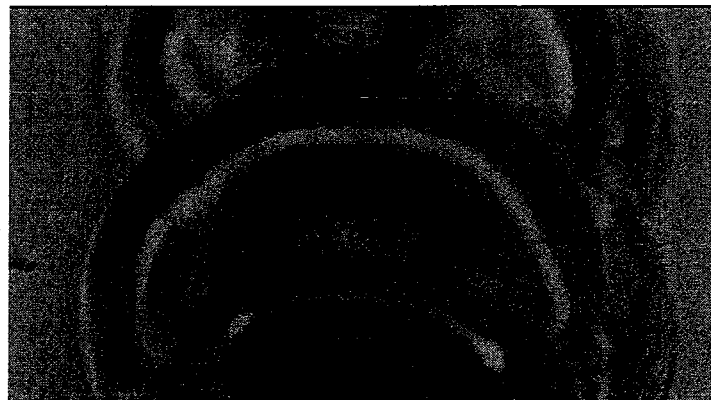
(b) Jagged out line contours with smooth channel surface



(c) Heat affected edges with smooth channel surface



(d) Heat affected edges with rough channel surface



(e) Deteriorated micro-channels

Figure 2-2. Channel contours

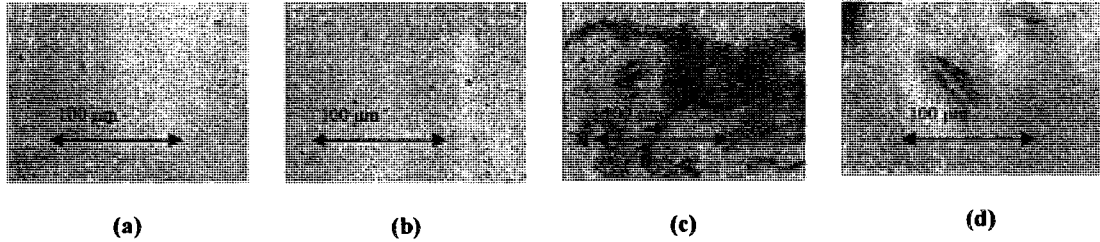


Figure 2-3. Quality of the surface of machined micro-channels, (a) Channel surface for well defined edge (b) Channel surface for jagged edge, (c) Channel surface for heat affected edge, (d) Rough channel surface with heat affected boundaries

2.2.2. Geometry of machined micro-channels

There are two main parameters in investigation of the geometry of the machined micro-channels: width and depth of the micro-channels. For a cylindrical stainless steel tool of 0.5 mm in diameter used in all of the experiments, the width for all the micro-channels was measured to be approximately 700 microns. But the depth of the micro-channels varies as a function of all the mentioned parameters in section 2.2. In the following, the effect of these parameters on the micro-channels depth will be discussed.

2.2.2.1. Machining depth as a function of time with constant applied voltage and speed

According to the experiments, the depth of the machined channels varies as a function of time. Considering the machined channels on a working piece, the depth of the fourth micro-channel is more than the third one and so on. For a precise study of this effect an experiment was performed at tool speed of $5\mu\text{m/s}$ for a micro-channel of 15mm length which lasted 50 minutes. Figure 2-4 shows the depth along different points of this micro channel as a function of time required to machine this length. The results show that there

is a meaningful relationship between the machining time and channel depth. As can be seen in figure 2-4, micro-channel depth increases as a function of time with a constant rate. The main contributor to this phenomenon seems to be chemical etching. Chemical etching increases with a constant rate, depending on the applied voltage and tool speed. This has been explained in section 2.4.2 in more detail.

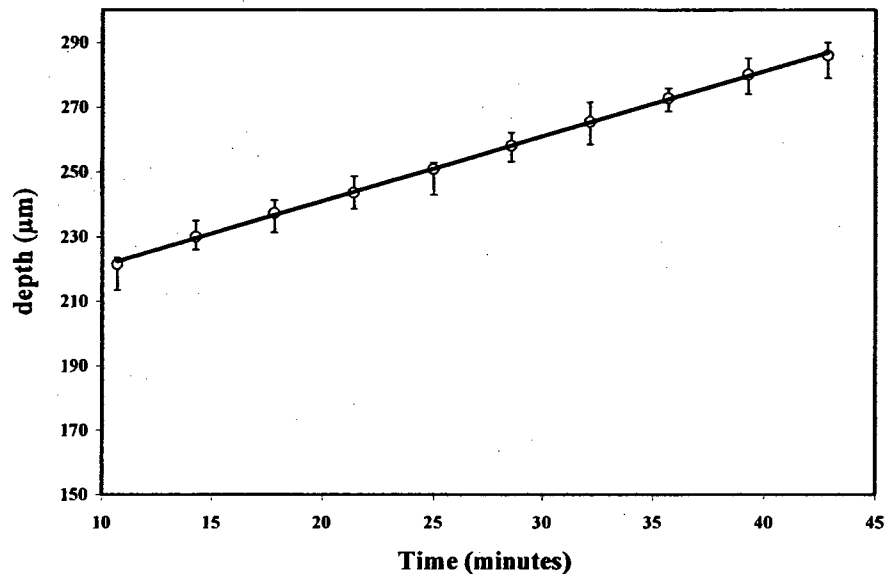


Figure 2-4. Micro-channel depth as a function of machining time in 28V and 5 $\mu\text{m/s}$. Standard deviation calculated from a batch of 4 experiments.

2.2.2.2. Depth of machined micro-channels as a function of voltage with constant applied speed

Higher voltages result in higher micro-channel depth. This statement is true up to 32V. Applying voltages higher than 32V at low speeds, as discussed in section 2.2.1, will not result in deeper micro-channels, but at high tool speeds, increasing the voltage results in

deeper micro-channels which follow the same geometry as in voltages less than 32V.

Figure 2-5 shows the effect of the increasing voltage at constant speed. This figure indicates the increasing trend of micro-channel depth with voltage.

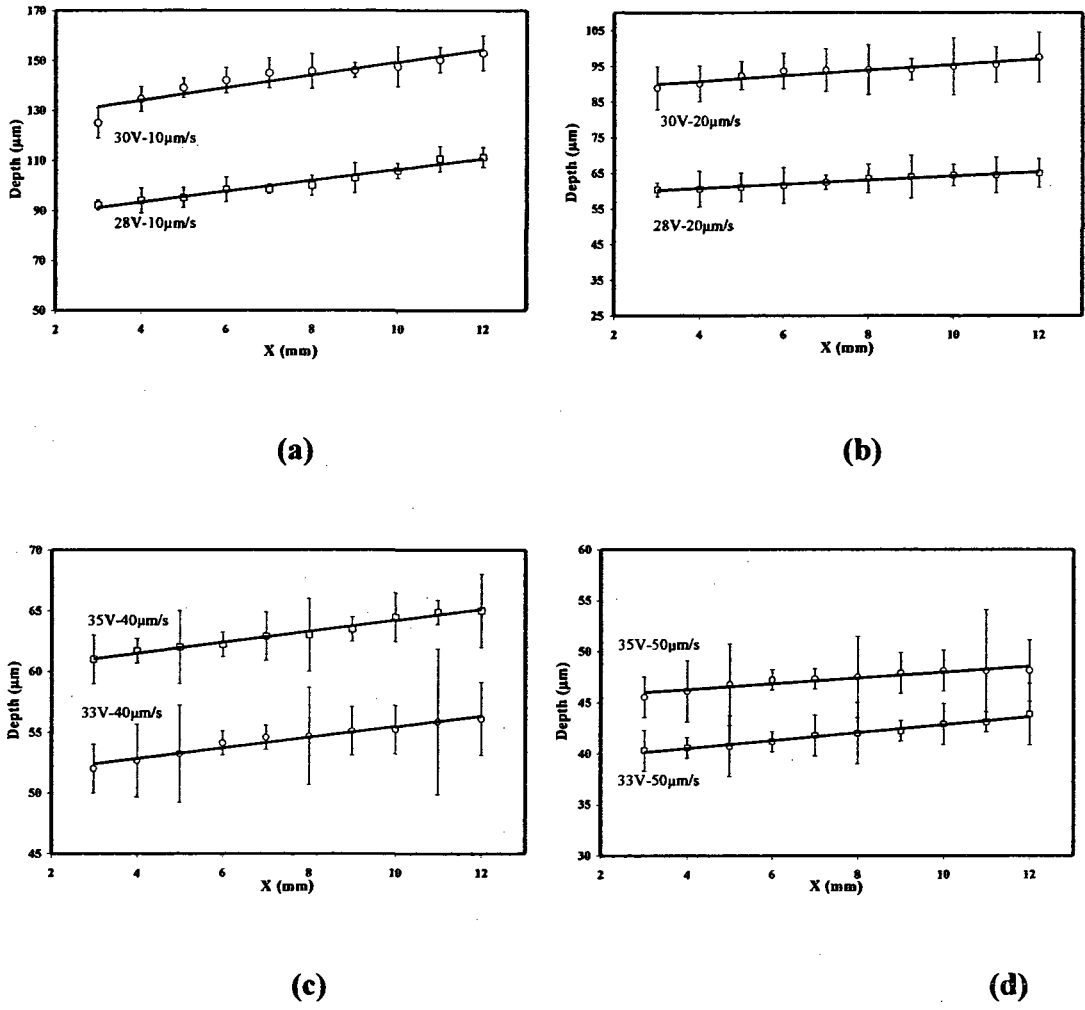


Figure 2-5. Micro-channel depth profile: (a) 28V and 30V at 10μm/s, (b) 28V and 30V at 20μm/s, (c) 33V and 35V at 40μm/s, (d) 33V and 35V at 50μm/s. Standard deviation calculated from a batch of 4 experiments.

2.2.2.3. Depth of machined micro-channels as a function of speed with constant voltage

Horizontal tool speed plays the main role in micro-channel depth. Decreasing the speed in constant voltages, results in deeper micro-channels as shown in figure 2-6. Initial depth ($x=0$) as a function of tool speed is shown in this figure in order to eliminate the effect of machining time on micro-channel depth. At 28V, tool speeds more than 40 $\mu\text{m/s}$ result in deteriorated micro-channels. Therefore, the mean depth curve for 28V has no meaning at speeds more than 40 $\mu\text{m/s}$.

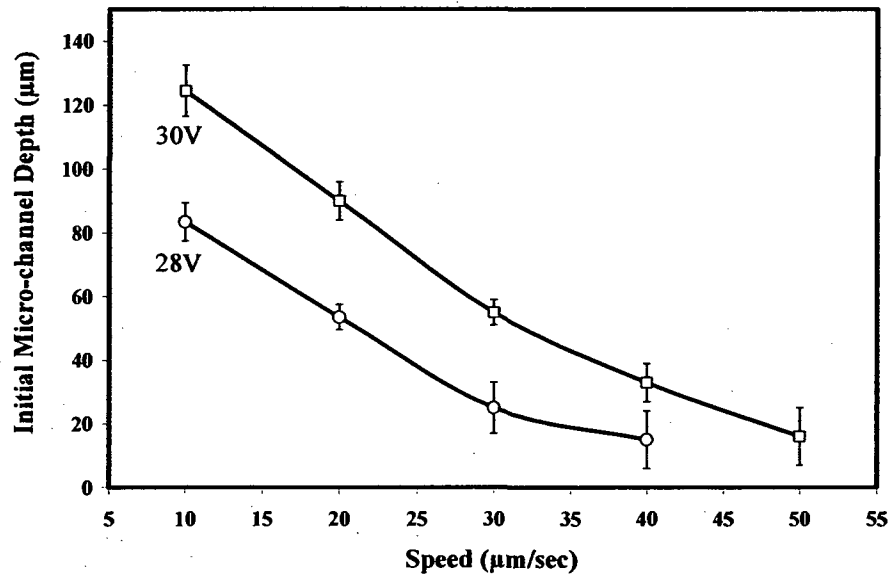


Figure 2-6. Initial micro-channel depth in 28V and 30V as a function of tool speed. Standard deviation calculated from a batch of 5 experiments.

2.2.2.4. Influence of tool distance from working piece

As discussed before, 2D-micro-machining yields acceptable results when the tool is kept at a distance of less than 25 microns from the glass surface [3]. To study the effect of tool distance on micro-machining performance, several experiments were performed by

varying the tool distance from the glass surface. Figure 2-7 shows the depth profile of the micro-channel machined at 30V and 30 $\mu\text{m/s}$ tool speed obtained with different tool distances from the glass surface. The average depth of the micro-channels is observed to decrease with increasing the tool distance. The quality of machined micro-channels does not change significantly for tool distances up to 15 μm and, depending on the machining voltage and tool speed, the same counters explained in section 2.2.1 are observed. For tool distances more than 15 μm , independent of the applied voltage and speed, the micro-channel counters tend to deteriorate as explained in section 2.2.1.

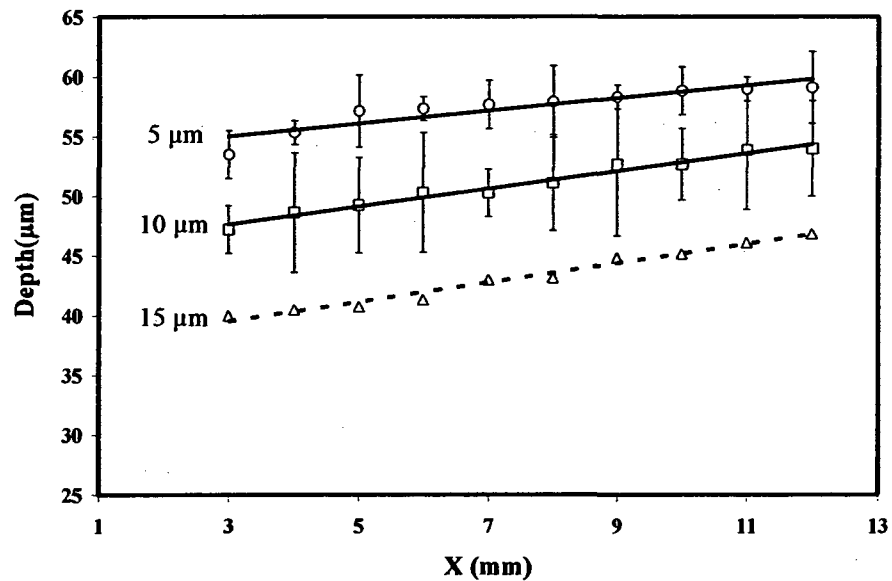


Figure 2-7. Micro-channel depth profile at different tool distances from glass surface (Machining voltage: 30V and tool speed: 30 $\mu\text{m/s}$), Error bars for 15 μm distance are omitted to improve illustration. Standard deviation calculated from a batch of 4 experiments.

2.3. Proposal of a model for micro-channels quality as function of voltage and speed

According to the experimental results discussed in the previous sections for 2D-micromachining with constant velocity using SACE technology, a model based on the

observed phenomenon is proposed. Micro-channel fabrication can be divided into five regions in the voltage and tool speed plane, as shown in figure 2-8.

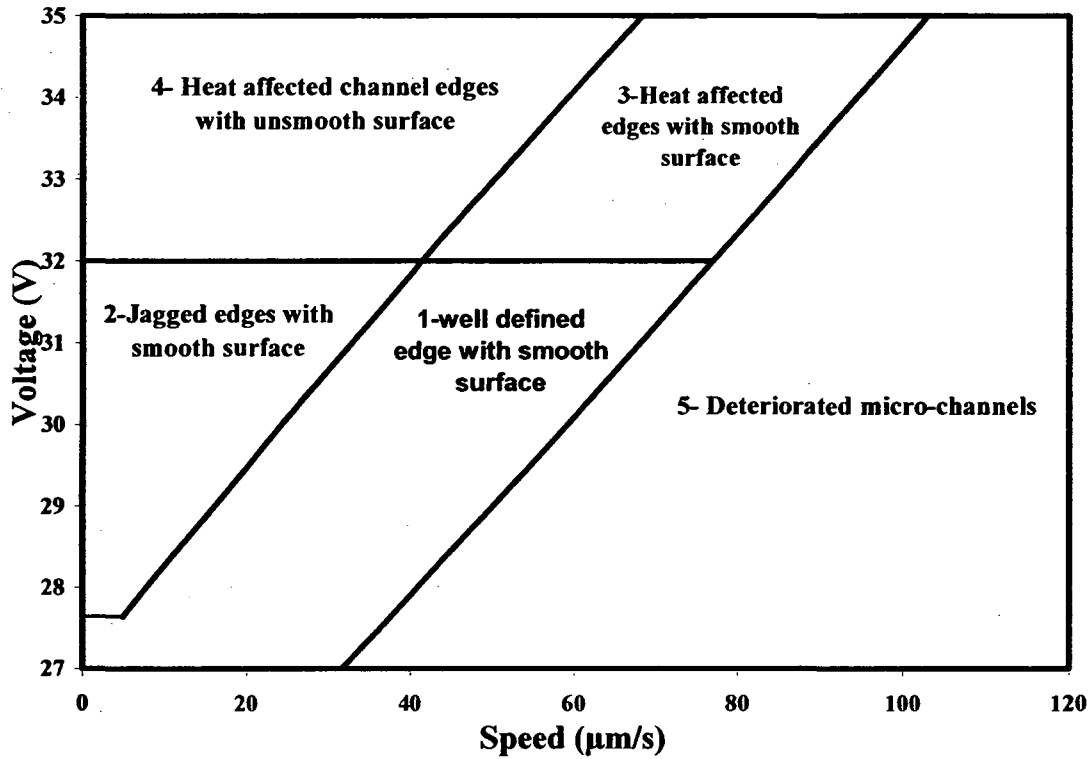


Figure 2-8. Characterization diagram proposed for micro-channels machined by SACE technology as a function of applied voltage and speed (for tool distance less than 15 μm).

It is observed that voltages less than 32V result in better micro-channel quality. In this voltage range, appropriate selection of tool velocity will result in the best micro-channel quality (region 1) in which channel depth varies between 50 to 120 microns depending on the applied parameters. Lower velocities will result in deeper micro-channels but the quality of the micro-channel edges will not be as good as region 1, although the micro-channel surface quality is still excellent. It should not be neglected that decreasing the speed will change the micro-channel depth smoothly because of the effect of time. So if

the aim is to have a micro-channel with the best quality and a constant depth of around 60 microns the best choice is to apply 28V at 20 $\mu\text{m/s}$ speed. In voltages less than 28V which results in a different electrochemical discharge regime, perfect edge and surface quality are obtained even at tool speeds less than 5 $\mu\text{m/s}$. This effect has also been reported for micro-hole drilling by gravity feed [5] and constant feed [28].

In voltages more than 32V the quality of the micro-channel edges are always heat affected. In this range if the velocity is chosen high enough, it is possible to have smooth micro-channel surfaces which have been indicated as region 3 in figure 2-8. On the flip side decreasing the tool velocity corrupts the micro-channel surface and results in very bad surface quality (region 4). As mentioned before, this seems to be because of the accumulation of the removed material inside the micro-channel area and inability in removing of the material from micro-channel surface. A schematic diagram of this process is shown in figure 2-9. This is represented by region 4.

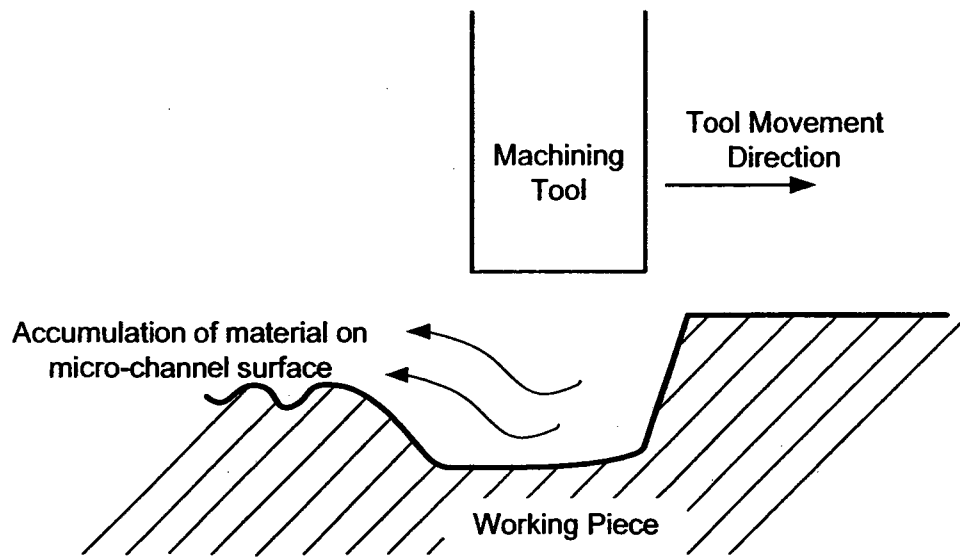


Figure 2-9. Schematic representation for accumulation of removed material on micro-channel surface for higher voltages at low speeds (region 4).

Finally, region 5 in figure 2-8 is a result of excessive speed. In this region there is not enough time for the glass to be removed and form an acceptable micro-channel. As the tool is moved above the glass surface with high speeds (region 5), it is possible to see the effect of the tool on the glass during the machining (figure 2-2(e)). In this region machined micro-channels look like discrete rings with 700 μm diameter. When the tool is moved along the micro-channel at lower speeds, these discrete rings combine together to form a continuous micro-channel.

In 2D-micro-machining with constant velocity the machining takes place mostly in the discharge regime and rarely in the transient regime. The width of the micro-channels for a stainless steel tool of 0.5mm in diameter is approximately 700 μm which is 100 μm more than the radius of the tool for each micro-channel edge. This number is reported to be around 80 microns by Maillard *et al.* [5] for the micro-holes drilled with gravity feed

technique in the discharge regime using a stainless steel tool of 0.4mm diameter [5]. The drilled micro-holes not deeper than 100 μ m (discharge regime) have well defined cylindrical contours with smooth surface[5], but in 2D-micromachining as shown in figure 2-8, the quality of the micro-channels depend on the applied voltage and speed (increasing the voltage or decreasing the speed, results in heat affected or jagged edges), even though machining happens in the discharge regime. This difference between the quality of the obtained micro-holes and micro-channels, which are both machined in the discharge regime, may be attributed to the fact that in the 2D-micro-machining with constant velocity, the tool is always moved in a certain distance from the glass surface which, in high voltages or low speeds, can destroy the quality of the edges. The main similarity between the proposed model for 2D-micro-machining with model proposed for micro-holes is the specific voltage in which significant difference is observed in the quality of the edges. This voltage in both models is equal to 32V.

2.4. Comparison of experimental data with theory

2.4.1. Heat transfer model and experimental results

Investigation of the time needed for the glass surface to start machining is very important. In this section the experimental results are interpreted based on the hypothesis that melting is responsible for the mechanism of material removal or the machining starts at the so called melting temperature. In figure 2-8, boundary of region 5 (deteriorated micro-channels) shows the tool speed at which the glass surface starts to melt for a specific voltage. The time needed for melting the glass surface assuming one dimensional heat transfer with constant homogenous heat source on the glass surface, can be approximated according to equation (2-1) [29].

$$(2-1) \quad \bar{T}(z=0, \bar{t}_0) = \sqrt{\bar{t}_0} \left[\frac{1}{\sqrt{\pi}} - \frac{1}{\sqrt{\pi}} e^{-\frac{1}{\bar{t}_0}} + \frac{1}{\sqrt{\bar{t}_0}} \operatorname{erfc} \left(\frac{1}{\sqrt{\bar{t}_0}} \right) \right] = \frac{1}{\kappa}$$

Simplifying equation 1 to find \bar{t}_0 results in:

$$(2-2) \quad \bar{t}_0 = \frac{b^2}{4a} \frac{k^2}{\pi(\kappa-1)^2}$$

Where a is the thermal diffusivity of glass, b is the tool radius and κ is the ratio between applied heat power and the minimal heat power necessary for machining.

The velocity required to melt a specific length of the glass surface (b' which is about 25 μm according to figure 2-2e) is:

$$(2-3) \quad V = \frac{b'}{\bar{t}_0}$$

Equation (2-3) indicates the speed in which the glass surface starts to melt. This speed is a representation of the boundary between well defined micro-channels with smooth surface (region 1 in figure 2-8) and deteriorated micro-channels (region 5 in figures 2-8). Figure 2-10 shows how this simplified heat model is capable of predicting the results for the boundary between regions 1 and 5 proposed in figure 2-8. According to the experimental data presented in figure 2-8, there is a jump in tool speed around 32V. This jump is most probably related to different regimes of electrochemical discharge and gas film formation. Further studies are needed to investigate it.

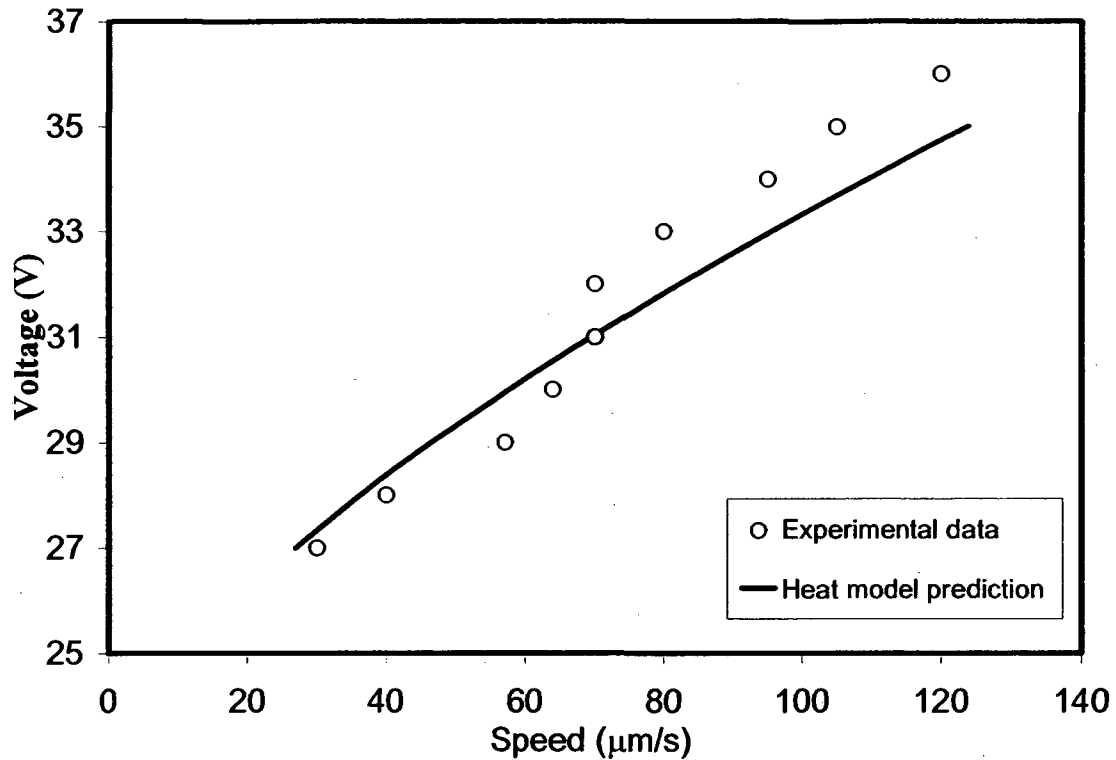


Figure 2-10. Comparison between experimental data and proposed theoretical model for speed limit needed to have micro-channel formation

2.4.2. Chemical etching model and experimental results

As discussed in previous sections, micro-channel geometry has a specific depth at the beginning of machining and this depth increases with time. Two mechanisms can be proposed for material removal. In the first mechanism the initial depth of the micro-channels are due to melting of the glass surface and increasing trend in micro-channels depth is because of chemical etching. Alternatively, machining may happen mainly because of chemical etching at high local temperature. The proposed chemical etching model in this chapter is based on the first mechanism and the second mechanism will be discussed in chapter 3. Therefore here we assume that as the machining starts, high temperature melts the glass surface and machines the surface to a specific depth

depending on the applied voltage and tool speed. This depth is retained at a constant level along the channel if the only phenomenon contributing to the machining process were physical melting of the glass surface. However, high local temperatures will increase the rate of chemical etching, making it a significant contributor to the machining process. Experimental data from Fascio [30] shows the relation between glass etching rate and applied temperature as illustrated in figure 2-11.

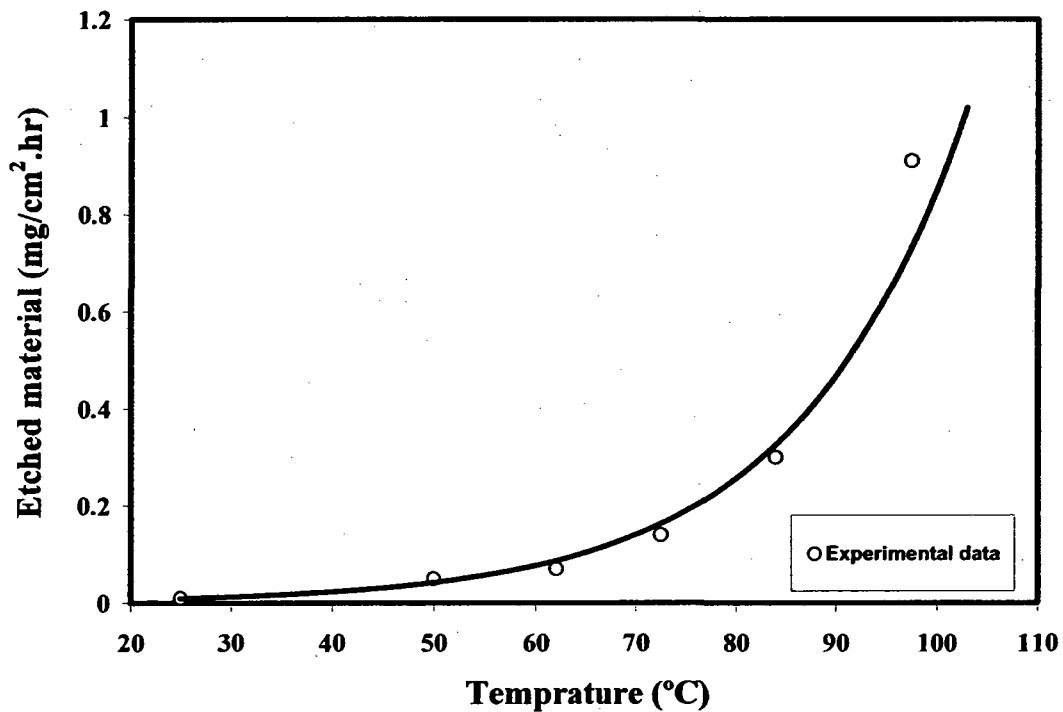


Figure 2-11- Chemical etching in different temperatures according to Fascio [30]

Fitting the experimental data in figure 2-11 to Arrhenius equation form, results in the following equation:

$$(2-4) \quad m = 3 \times 10^7 \exp\left(-\frac{6571.3}{T}\right)$$

Where m is the mass of the material removed in one hour per unit area of the glass and T is the etching temperature. As discussed in section 2.2.2.1, there is an increasing trend in micro-channels depth with time. Increasing rate in micro-channels depth for different tool speeds has been shown in figure 2-12a. According to this figure, the increasing rate for micro-channel depth varies as a function of applied voltage and tool speed. Applied voltage, as a representation of the heat transferred to the glass surface, and tool speed, as a representation of the time in which the tool remains above a specific point, both affect the local temperature of the glass surface. As the thermal energy (applied voltage) or the duration of heat transfer increases (tool speed decreases), the local average temperature at which the chemical etching reaction happens, will increase. Therefore chemical etching rate will also increase according to equation 2-4. Figure 2-12b shows this temperature variation for 28V in different speeds.

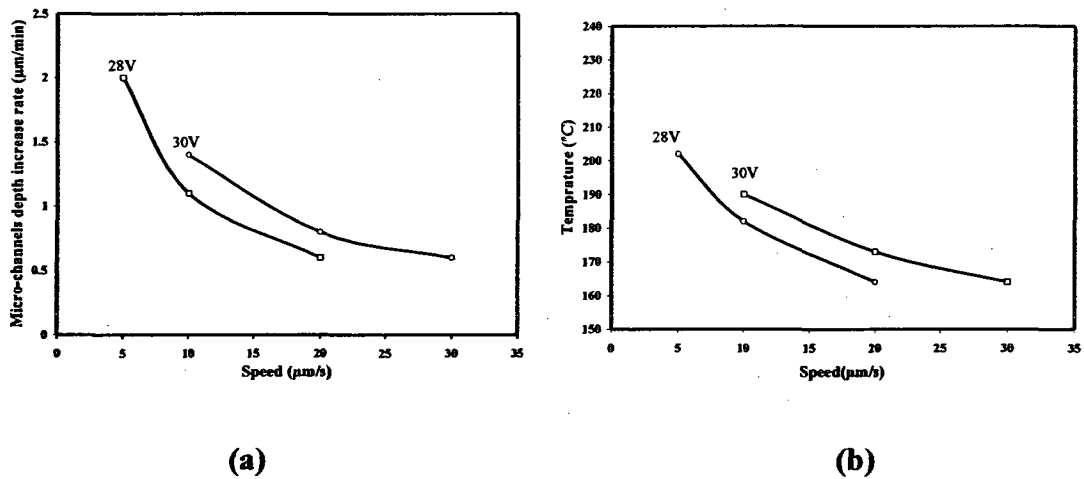


Figure 2-12-a) Increase in rate of micro-channel depth as a function of tool speed in different voltages b) Predicted local chemical etching temperature in 28V and 30V for different tool speeds

According to Fascio [30] at constant temperature, mass removed from the glass surface by chemical etching increases with a constant rate. Our experimental data illustrated in

figure 2-12a also shows that increasing rate in micro-channel depth is constant for each specific applied voltage and tool speed. So the constant increasing rate in machined micro-channel depth can be attributed to the chemical etching which happens at constant temperature. Figure 2-12a can be used to control the tool motion in order to cancel the chemical etching effect on the depth of the micro-channel.

2.5. Conclusion

In this chapter parameters affecting the quality and geometry of the micro-channels machined by SACE technology with constant velocity were presented and the effect of each of the parameters was assessed. Meanwhile, using a cylindrical tool with 0.5mm diameter, the micro-channel width remains constant, around 700 microns, their depth can vary between 50 to 300 μ m depending on different parameters. Best micro-channel quality with desired depth can be achieved at voltages less than 32V and tool velocity less than 30 μ m/s at tool distance less than 15 μ m from the glass surface.

Five types of micro-channels were obtained:

1-Well-defined linear micro-channel edges and smooth channel surface

2-Jagged out line contours with smooth micro-channel surface

3-Heat affected edges with smooth micro- channel surface

4-Heat affected edges with unsmooth micro-channel surface and thermal cracks

5-Deteriorated micro-channels

The presented qualitative model with achievable geometrical properties of the micro-channels, using SACE technology with constant velocity, is a new approach for 2D-micro fabrication which can be used in a lot of applications especially in fabrication of microfluidic and Lab-on-a-Chip devices.

Results from the experiments in this chapter drew attention to several interesting phenomena such as the effect of chemical etching on machining with SACE technology. The contribution of chemical etching to micro-machining with SACE will be discussed in chapter 3.

3. Material Removal Mechanism

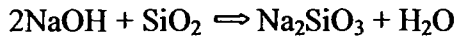
This chapter provides a quantitative description of the material removal mechanism in SACE micro-machining. The parameters that affect material removal in SACE are assessed and electrolyte concentration is chosen as the main variable parameter to investigate the chemical effects in SACE process. Therefore the experiments were performed under a range of different electrolyte concentrations, keeping the other parameters constant. The mechanism of material removal is investigated based on the quantitative and qualitative characterization of 2D-micro-machining by using different electrolyte concentrations and analyzing the machined samples and the used electrolyte after machining. The amount of silicon inside the electrolyte after machining is investigated by Inductive Coupled Plasma Mass Spectrometry (ICP-MS) test. The ICP-MS test performed on the electrolyte before and after machining, showed that significant amount of silicon is being added into the electrolyte during machining. This was found to be in accordance with the recorded removed mass of the machined samples. Finally, analyzing the experimental results, it is concluded that the main contributing phenomenon to material removal is chemical etching at high local temperatures.

This chapter is based on the following publication:

Fatanat Didar T., A. Dolatabadi, R. Wuthrich, *Chemical contributions to the mechanism of patterning micro-channels and micro-holes on glass substrates with Spark Assisted Chemical Engraving (SACE) Technology*, to be submitted to **Materials Chemistry**, 2008.

3.1. Chemical etching in SACE micro-machining

In case of glass machining using sodium hydroxide, the work-piece is etched by formation of silicate according to [3]:



The formed sodium silicate dissolves in the electrolyte. This chemical reaction is strongly enhanced by increasing the temperature [31]. Similar results are reported for ceramic materials [32]. In case of quartz machining, a similar process was suggested by Jain *et al.* [33].

Very first evidence about chemical effects comes from the comparison between SACE machining using a negatively and positively polarized tool-electrode. The polarity of the electrode-tool influences the machining process [27, 33]. It was shown first by West *et al.* [34] that using an active anode as tool-electrode during drilling, the shape of the drilled hole is spherical compared to cathodic machining where it is conical. Even the exact mechanism is not yet elucidated; a possible contribution to the explication could be the following: when using an anode tool-electrode, the electrochemical discharges are no longer carried by the electrons but by ions. As explained by Hickling and Ingram [35] ions are bombarding the gas film-electrolyte interface resulting in the production of OH radicals by the decomposition of water. Therefore, the concentration of OH radicals as a function of the hole depth, z , is more or less uniform. The work-piece is etched isotropically resulting in a spherical shape (Figure 3-1). This situation changes when using an active cathode as tool-electrode. In this case only OH radicals from the electrolyte (NaOH) are present. During machining, the electrolyte is mainly present at the

top of the hole. The concentration of OH radicals decreases with z resulting in a larger entrance diameter. This mechanism will result in a conical micro-hole shape.

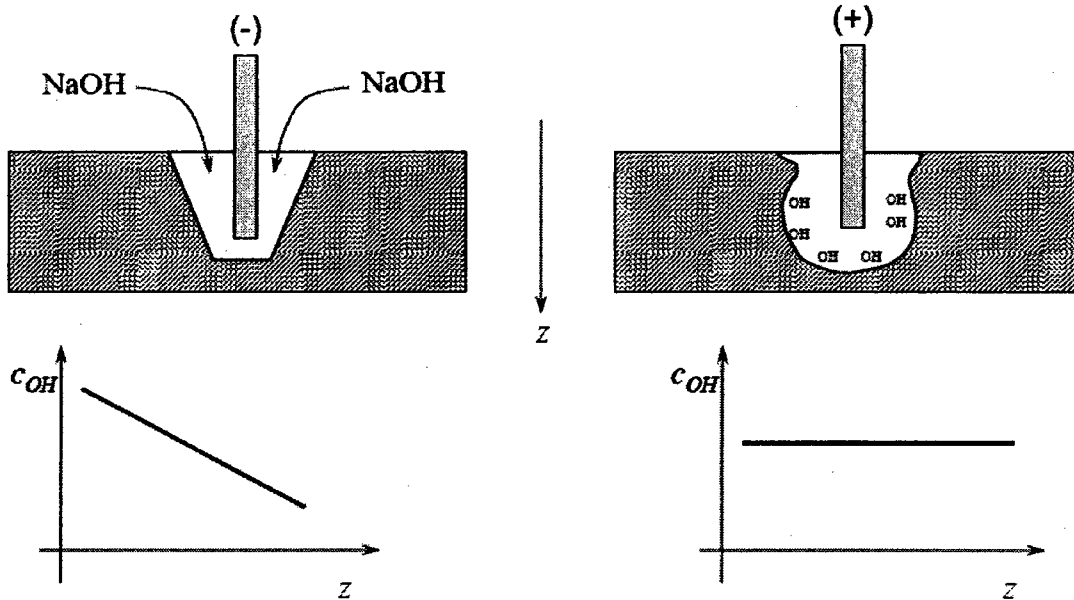


Figure 3-1-Comparison of machining with an active cathode and anode. In case of an active anode, the Hickling Ingram mechanism will produce a uniform OH concentration along the hole resulting in a spherical shape whereas in the case of a cathode-tool, the concentration of OH ions decreases with the hole depth resulting in a conical shape [33]

More OH radicals are present during anodic machining, thus chemical etching is expected to be more important in this case. Consequently, the surfaces are smoother than those with cathodic machining [33, 34]. However, when using an anodic polarization, the tool-electrode gets anodically dissolved resulting in high tool wear.

3.2. Parameters affecting the material removal mechanism

As discussed before, local melting and chemical etching are known as the main factors for the material removal mechanism in SACE. Several machining parameters affect the material removal, the most important of which are electrolyte concentration, applied

voltage and in case of 2D-micro-machining the tool speed. Varying these parameters influences either the time or the amount of the thermal energy exposed to the sample's surface, which can both affect the melting and the rate of chemical etching. For example, increasing the applied voltage will result in more thermal energy exposure on the surface which can cause more melting and also increase the chemical reaction's rate. Therefore it is important to choose appropriate parameters and perform the experiments in the way that can clarify the effect of the chemical etching in the process. The aim is to find a machining parameter that, when varied, changes the chemical reactions rate while keeping the amount of exposed energy as constant as possible. For this purpose, concentration of the electrolyte is chosen as the main parameter and thus varied over a wide range while keeping all the other parameters constant. It could be argued that the concentration of the ions inside the electrolyte might affect the energy exposure on the surface; however this argument is ruled out by the experimental results which fully confirm choice of the main parameter and will be discussed in section 3.4.5.

3.3. Experimental Procedure

It is possible to drill micro-holes or machine micro-channel with SACE technology on glass samples, but in order to have a clear understanding of the material removal mechanism, in this study; we have applied 2D-micro-machining with micro-channel patterns. The main reason for this choice is that with a micro-channel pattern, it is more convenient to investigate the time dependent changes in geometrical characteristics of the pattern. Therefore, the 2D-micromachining technique with constant velocity was applied. In this technique, the machining tool is moved with a constant speed and constant

distance from the glass surface. Detailed description of the 2D-glass micromachining with constant velocity was discussed in chapter 2 [4].

The experimental procedure, consisting of five steps, is as follows:

- a) Cleaning of glass samples (Soda lime glass) in an ultrasonic bath for five minutes with acetone followed by mass determination with an analytical balance (0.1mg precision)
- b) 2D-micro-machining with a 40mm long micro-channel pattern according to the procedure described in chapter 2 [4].
- c) Cleaning of machined samples in an ultrasonic bath with subsequent mass measurement
- d) Performing FT-IR analysis on machined micro-channels.
- e) Performing ICP-MS test on the electrolytes (NaOH) before and after machining for measuring the amount of removed material

The electrochemical discharge regime was also investigated during the machining process using a 50 MHz current probe.

The electrolyte used is aqueous sodium hydroxide solution (10, 20, 30 and 40 wt%) prepared from NaOH purchased from Sigma Aldrich and deionized water. The electrolyte was heated up to 80 °C before starting the experiments. The machining tool was a cylindrical electrode of 0.5 mm in diameter made of 316L stainless steel. As a counter electrode, a large cylindrical ring (same diameter as the processing cell) of stainless-steel was used. The work-pieces were standard glass sample holders for optical microscopes

which were described in chapter 2. The processing cell and the power source are the same as in chapter 2.

In order to achieve micro-channels with good quality, the machining speed was chosen to be 5 μ m/s and the applied voltage to be 28V [4]. To better quantify the increasing trend in micro-channels depth, the length of the micro-channels were chosen to be the maximum possible length (40mm).

3.4. Results and discussions

The machining parameters were chosen to achieve the best micro-channel quality (well defined edges with smooth micro-channel surface as described in chapter 2 and [4]). In all experiments machining parameters are kept constant, but the main contributor to the chemical effects, electrolyte concentration, is varied in different experiments. Varying the electrolyte concentration while all other parameters are kept constant is expected to reveal the chemical effects on the material removal mechanism. In the following the results from two different sets of experiments are presented and discussed: 1) the quality and geometry of micro-channels resulting from performing 2D-micro-machining with different electrolyte concentrations and 2) analyzing the machined samples and the used electrolyte after machining.

3.4.1. Depth profile variation with electrolyte concentration

According to the experiments, the depth of the machined micro-channels varies as a function of electrolyte concentration. The initial depth of the micro-channels increases with the electrolyte concentration. Figure 3-2 shows the initial depth of the micro-channels machined with different electrolyte concentrations. The results show that there

is a meaningful relationship between the electrolyte concentration and micro-channels initial depth. This increasing trend varies with different electrolyte concentrations.

Figure 3-3 shows the slope of the micro-channel depth profile obtained with different electrolyte concentrations. As can be seen in figures 3-2 and 3-3, the initial depth and slope of the depth profile increases with the electrolyte concentration. Two main factors may have contributed to this increase, first being that the discharge activities can change using different electrolyte concentrations. By increasing the concentration of the ions inside electrolyte, the critical voltage might change. As mentioned, the critical voltage is the voltage where a gas film starts to form around the electrode. Therefore fixing the machining voltage alone does not warranty the same amount of energy exposed to the glass surface and critical voltage is the key to insure the real amount of exposed energy. Critical voltage for different electrolyte concentrations will be discussed in section 3.4.5.

Second factor contributing to the increasing trend in micro-channels depth is chemical etching. This increasing trend in the initial depth and slope confirms the proposed statement that machining takes place mainly due to chemical etching at high local temperatures.

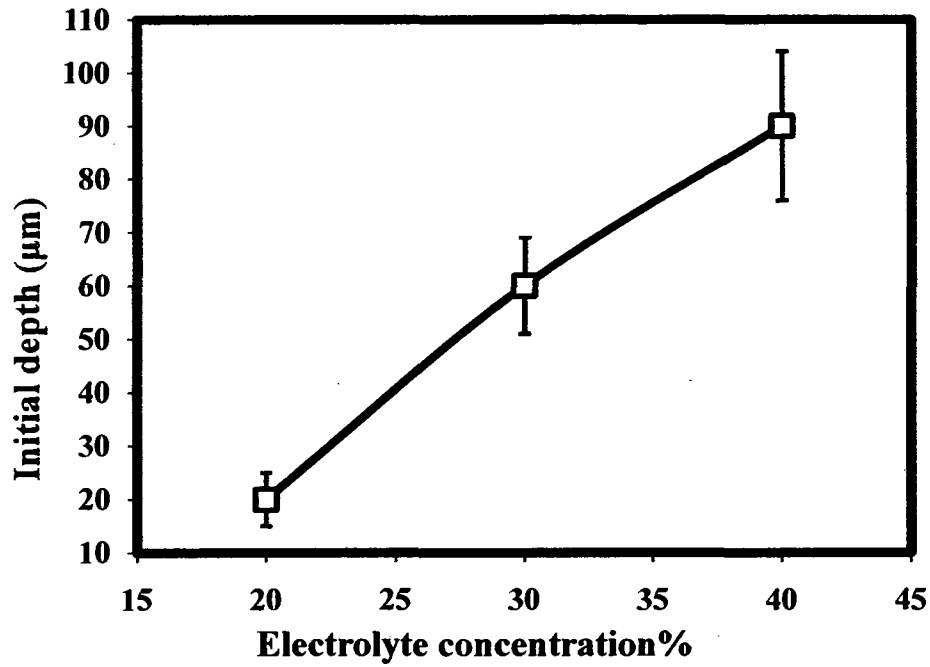


Figure 3-2. Initial depth of the micro-channels machined with different electrolyte concentrations (Tool speed: 5µm/s, Tool diameter: 0.5mm, applied voltage: 28V), Standard deviation calculated from a batch of 4 experiments.

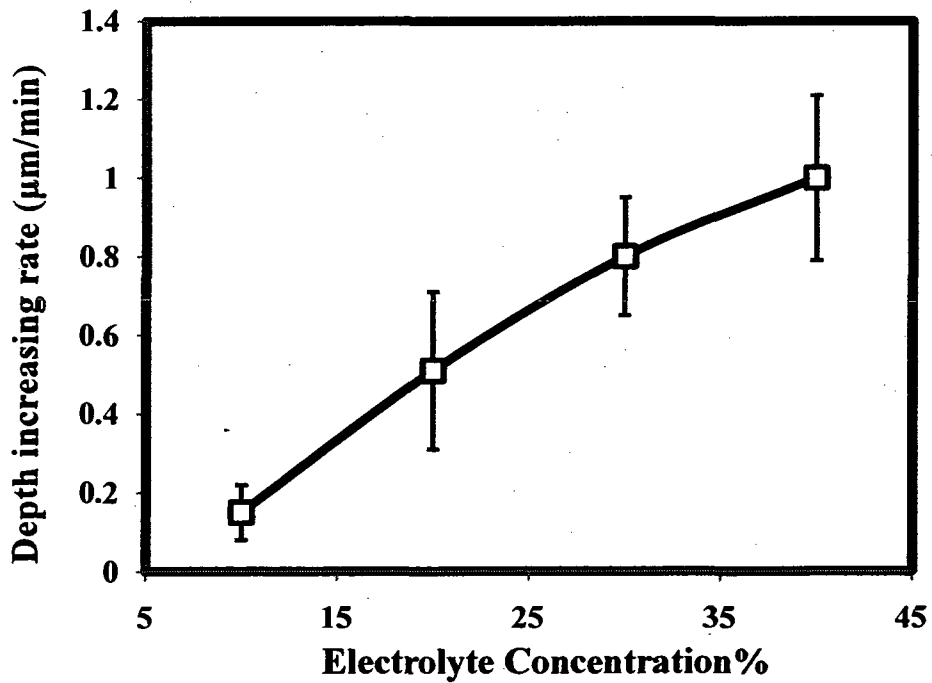


Figure 3-3. Increasing trend in depth profile of micro-channels along with different electrolyte concentration, Standard deviation calculated from a batch of 4 experiments.

3.4.2. FT-IR analysis of the machined samples

In a previous work FT-IR analysis on samples machined with 30% electrolyte concentration was performed [36]. Figure 3-4 shows the resulting FT-IR spectrum. The red spectrum represents the area of the microscopic slide glass surface which has not been machined but immersed in the electrolyte and the blue spectrum represents the machined area (i.e. channel). The roughness of the machined surface makes an FT-IR analysis difficult and the observed effect may not solely be attributed to the change of the chemical structure of the glass during machining. However the roughness effects were minimal in the sample machined with 30% electrolyte and the FT-IR results observed are an indication for the chemical change of the glass surface during machining. It is observed that the band associated with the antisymmetric Si-O stretch involving bridging oxygen (1100cm^{-1}) in Si-O-Si, has undergone changes in the channel area.

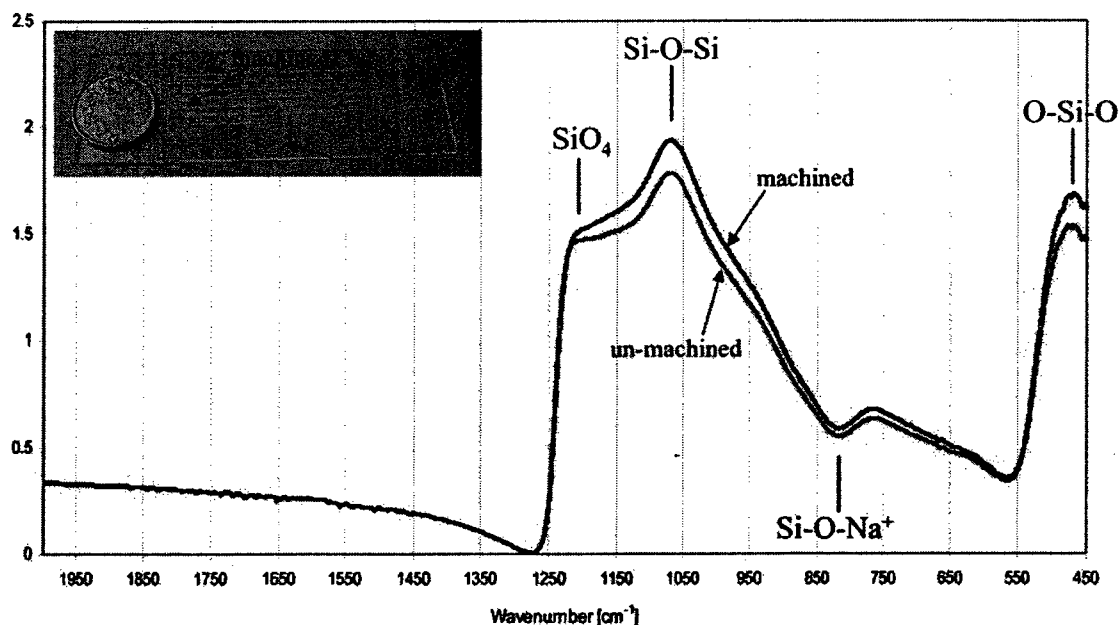
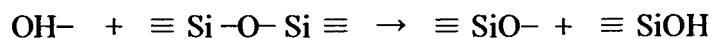


Figure 3-4. FT-IR analysis of the machined sample [36]

The band at 500 cm⁻¹ is subjected to the same changes as it represents complimentary bending band (O-Si-O). This is typical for the chemical etching by the OH⁻ radicals:



Changes of the Si-O-Na⁺ band (800-850 cm⁻¹) are not clear in this case, probably because sodium is already present in the glass.

3.4.3. Material removal assessment

To study the material removed from the glass surface, mass of one randomly selected sample for each electrolyte concentration was measured using an analytical balance. Figure 3-5 shows the removed material from glass surface measured by an analytical balance. It was observed that the removed material increases with the electrolyte concentration, which is similar to the observations discussed in section 3.4.1 for the depth of the micro-channels.

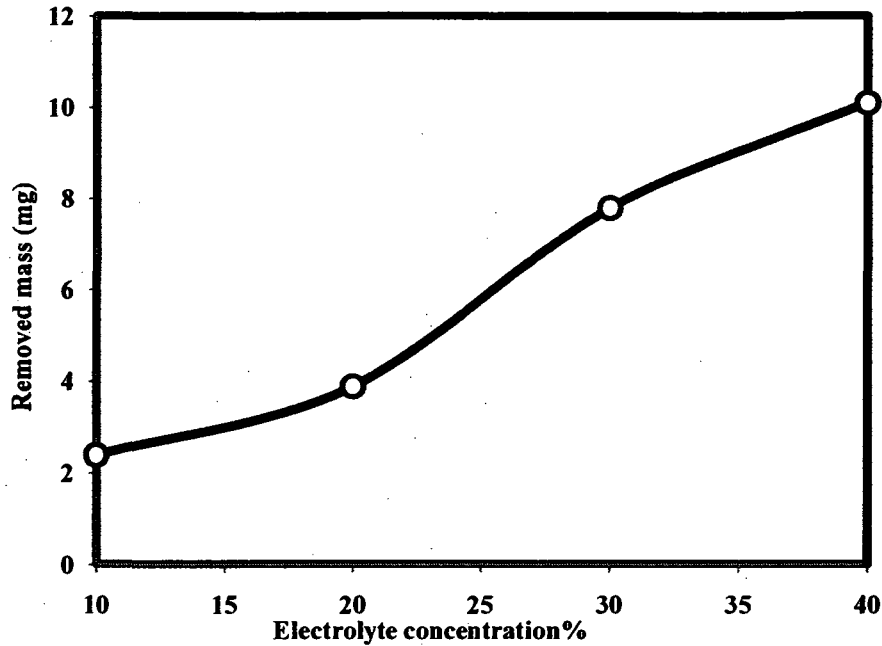


Figure 3-5. Material removed from the glass surface during 2D-micro-machining measured by analytical balance

3.4.4. ICP-MS test for silicone concentration inside machined samples

In order to find out the amount of the removed material from glass surface inside the electrolyte after machining, Inductively Coupled Plasma Mass Spectrometry (ICP-MS) tests were performed on the used electrolytes. 40 ml of 40 wt% sodium hydroxide solution was used for machining and then the concentration of silicon inside the used electrolyte was measured with ICP-MS tests. To perform the test, three solutions of silicon with 0, 1 and 5ppm concentrations were prepared and characterized for ^{28}Si , ^{29}Si , ^{30}Si . Then ICP mass spectrometry was performed on the 40 wt% electrolyte before and after machining. The electrolyte samples were diluted 50 times to achieve more accurate results. The number of counts for different silicon isotopes has been shown in table 3-1.

Table 3-1. Results of ICP-MS test on 40 wt% electrolyte (50 times diluted)

Si isotopes	Pure solution (Counts)	1ppm Si solution (Counts)	5ppm Si solution (Counts)	Electrolyte before machining (Counts)	Electrolyte after machining (Counts)
28	3288	7124	29233	4196	20100
29	155	437	1771	212	1671
30	2394	2683	3643	2864	3587

Based on the results from the ICP-MS test, about 140ppm silicone, equivalent to 5.5mg, is added to the electrolyte during machining. This amount shows that about 11.75mg of SiO₂ has been removed from the glass surface. The amount of removed material measured from sample mass difference, shown in figure 3-5 for 40% NaOH concentration, confirms the result from ICP-MS test.

3.4.5. Discharge regime and exposed energy in different electrolyte concentrations

As discussed in section 3.4.1, different discharge activities can cause variation of the initial depth and slope of micro-channels in experiments with different electrolyte concentrations. Therefore it should be clarified if the exposed energy to the glass surface varies in different cases or not. The exposed energy depends on the applied voltage and the critical voltage after which the gas film appears around the electrode [12]. Wuthrich *et al.* [37] reported the critical voltage for different electrolyte concentrations (Figure 3-6). At concentrations higher than 15%, critical voltage remains almost constant between 20 to 22V. The applied voltage is 28V in all experiments. Therefore the exposed energy for 20%, 30% and 40% electrolyte concentrations remains constant. The main conclusion is that the increasing trend in micro-channels initial depth and slope cannot be due to

different discharge activities. This confirms the statement that the mentioned variations are due to chemical etching.

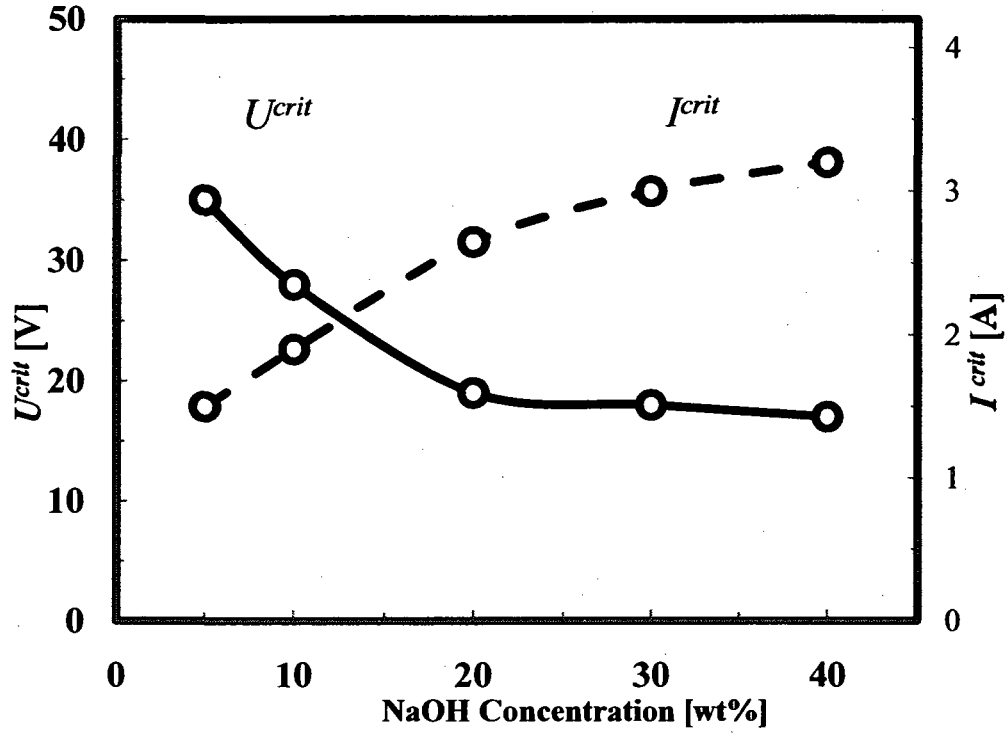
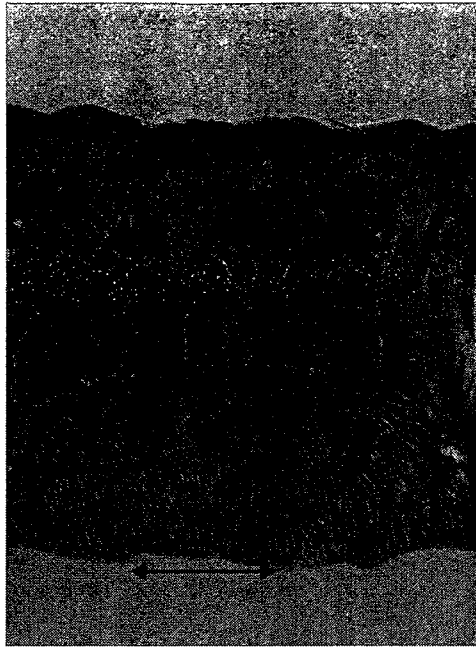


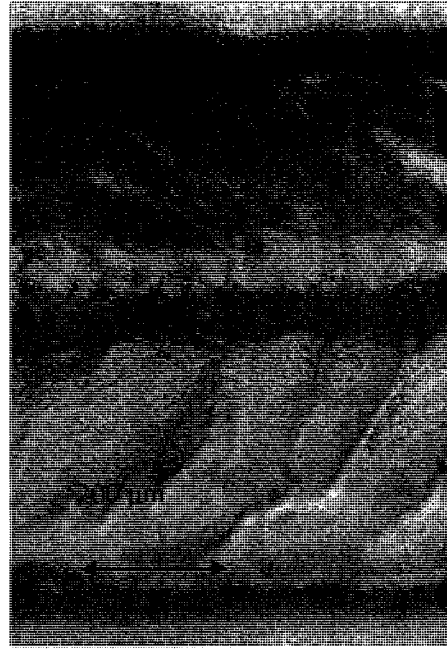
Figure 3-6. Critical voltage for different electrolyte concentrations [37]

3.4.6. Different micro-channel contours using different electrolyte concentrations

Different micro-channel contours are observed using various electrolyte concentrations. Figure 3-7 shows the surface of the machined micro-channels. The contour shown in figure 3-7a for 10% electrolyte concentration can be attributed to the electrical discharge effects and also the effects of the hydrodynamic regime during machining. Because of the lack of enough ions in this case, chemical etching seems to happen only in the discharge-exposed areas which experience higher temperatures. As the electrolyte concentration increases, a smoother micro-channel surface can be achieved. 30% electrolyte concentration results in the best surface quality. As shown in figure 3-7d, using 40% electrolyte concentration will extensively etch the surface in some areas which results in an unsmooth surface.



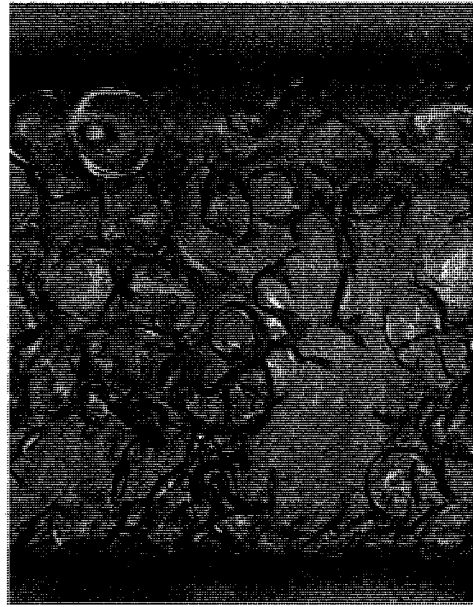
(a)



(b)



(c)



(d)

Figure 3-7. Micro-channel contours: a) 10% electrolyte concentration, b) 20% electrolyte concentration, c) 30% electrolyte concentration, d) 40% electrolyte concentration

3.5. Conclusion

In this chapter the material removal mechanism in SACE 2D-micro-machining was investigated through a set of different experiments. The results from the FT-IR analysis on the machined sample and ICP-MS test for the silicone concentration inside electrolyte after machining, confirm the presence of silicone inside the electrolyte after machining which, in turn, proves that material removal mechanism does indeed involve chemical etching. The increasing trend in material removed from the glass surface by increasing the electrolyte concentration, while keeping other parameters constant, showed that chemical etching at high local temperatures is the major phenomenon contributing to the machining process.

4. Glass Surface Modification by Electrochemical Discharges

In this chapter, the changes in glass density and hardness during machining are discussed. Based on the results from the experiments explained in chapter 3, there are some evidences that glass properties change after machining. To investigate these changes, the material removed from the glass surface, described in chapter 3, is evaluated by two different techniques and then nano-indentation test is performed on machined samples to confirm the changes. Based on the measured change in mass of the samples and results from nano-indentation test, it was found that hardness and density of the energy exposed areas after machining are less than unexposed areas of the samples. Etching the machined samples with HF shows that the energy exposed areas are etched with a lower rate which again confirms reduction in glass density.

This chapter is based on the following publication:

Fatanat Didar T., Dolatabadi A., Wuthrich R. *Local hardness and density variation in glass substrates machined with Spark Assisted Chemical Engraving (SACE)*, **Materials Letters** (2008), doi: 10.1016/j.matlet.2008.08.056.

4.1. Experimental procedure

Standard glass sample holders for optical microscope with a thickness of 1mm, (Menzel-Glässer, soda-lime glass) were used as working pieces to be machined with SACE technique. The experimental procedure, consisting of six steps is as follows (figure 4-1):

- a) Cleaning of glass samples in an ultrasonic bath for five minutes with acetone followed by mass determination with an analytical balance (0.1mg precision)
- b) 2D-micro-machining with a micro-channel pattern according to the procedure described in chapter 2. [4].
- c) Cleaning of machined samples in an ultrasonic bath with subsequent mass measurement and characterizing micro-channels geometry with an optical microscope.
- d) Preparation of sample for the nano-indentation tests by diamond saw cutting of the work-pieces
- e) Nano-indentation test on the micro-channel surface and the un-machined surface of the cut work pieces.
- f) Dipping the machined samples in 20v/v% HF solution for 20 minutes.

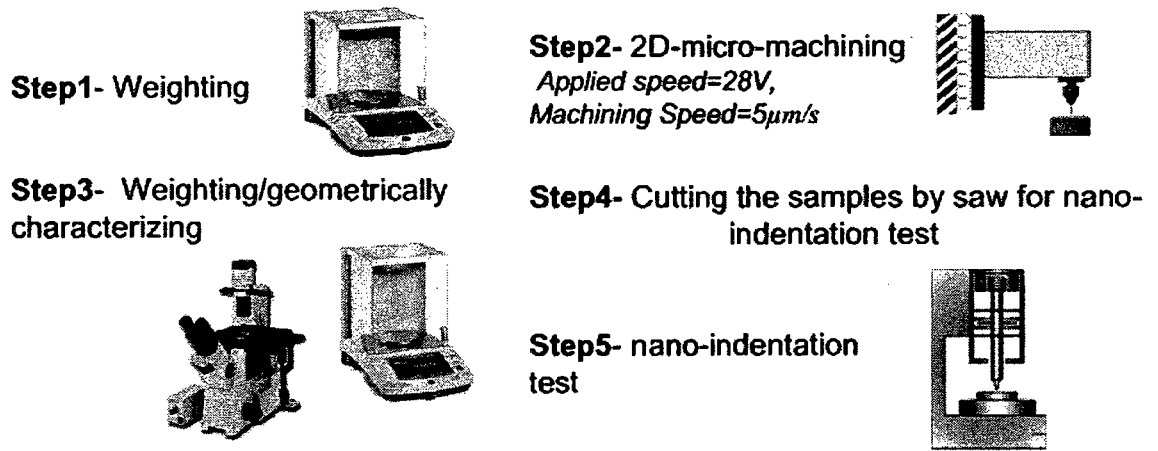


Figure 4-1. Schematic representation of the experimental procedure

In all experiments, sodium hydroxide with different concentrations (10, 20, 30 and 40wt %) was used. In order to achieve micro-channels with good quality, the machining speed was chosen to be 5 μ m/s and the applied voltage to be 28V [4]. For all the experiments a cylindrical, 0.5mm in diameter, stainless steel tool was used and the length of the machined micro-channels was 40mm.

The Nano-Indentation test was performed by load-controlled indentation using a Hysitron Nanoindenter with a Berkovich pyramid indenter (edge radius: >40 nm). The load was increased to 2000 μ N, kept constant at this value and decreased to zero, each stage taking five seconds. It was found to be hard to accurately align the tip of the nano-indenter inside the micro-channel surface. To overcome this issue the samples were placed in the nano-indenter such that the cross section of the micro-channel could be monitored by an optical microscope to assure that the tip touches the machined surface of the micro-channel.

4.2. Results and discussions

Removed material from samples surface was measured by two different techniques: 1) Using an analytical balance and 2) Based on the removed volume as calculated from the geometry of the machined micro-channels. In the second technique, the removed volume was calculated by using an optical microscope to identify the geometry of the micro-channels. Glass density was assumed constant before and after machining. Figure 4-2 shows the removed material from glass surface calculated by the two methods. The results are contradictory to what is expected: the two techniques yield to different figures for the removed mass.

The used analytical balance gives the mass of the samples with 0.1mg precision and the geometry of the micro-channels is determined with 1 μ m precision. The density of the samples (Soda lime glass) was calculated by gravimetric methods to be 2.45g/cm³. The density of soda lime glass in literature has been reported to be between 2.2 to 2.45gr/cm³ [38]. Therefore it is concluded that the measured data and thus the deviation of the obtained results from the two techniques are meaningful and not an artifact of the experiment.

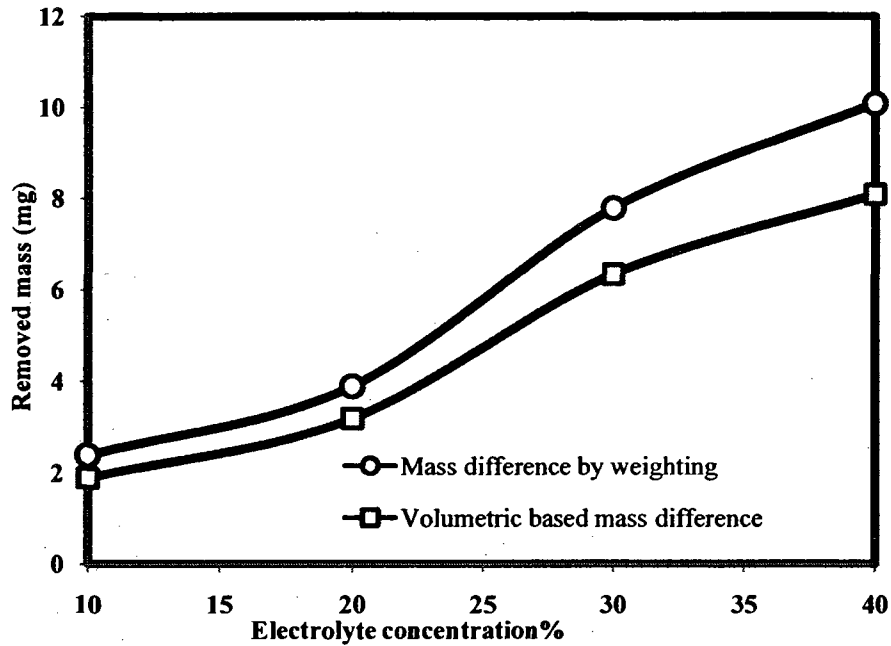


Figure 4-2. Material removed based on measuring samples weight before and after machining and based on calculated volumetric removed mass

The percent deviation of the removed mass calculated by the two methods is shown in table 4-1. This deviation is about 20% in all cases. This difference is attributed to the change in local density of glass in the machined areas. In order to confirm this change in glass property, the nano-indentation test was performed on the surface of machined micro-channels.

Table 4-1. Percent deviations for the removed mass calculations by two different techniques

Electrolyte concentration%	Percent deviation%
20	20.29
30	20.52
40	20.79

The nano-indentation test was performed on the free surface (un-machined area) of the glass sample five times in different points; the results show a hardness of 6.8 (± 0.1) MPa. The nano-indentation test was also performed on the machined micro-channels surface. The test for the micro-channels surface showed a hardness of 5.2 (± 0.5) MPa. Figure 4-3 shows the force-displacement graph of nano-indentation test inside and outside the micro-channel which was machined with 30wt% electrolyte concentration. This difference in hardness justifies the previous hypothesis about the change in the physical properties of machined substrate and shows that the material becomes softer after machining. This softness is a clear indication of changes in glass density.

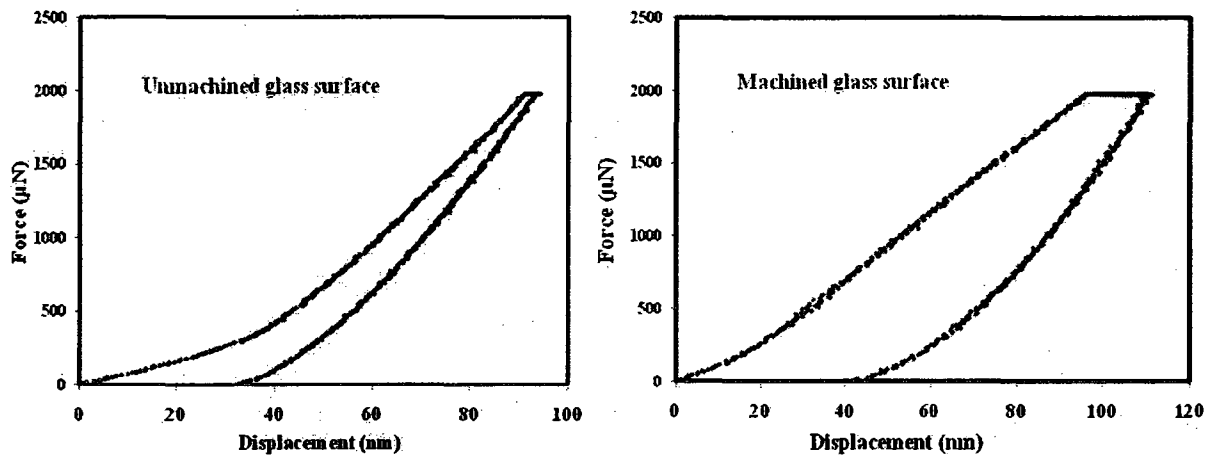


Figure 4-3. Force-Displacement graphs of nano-indentation test before and after machining using 30wt% electrolyte concentration

The percent deviation for the measured hardness of micro-channels surface and the hardness measured for the un-machined glass surface is about 23%. This is in the same range as the percent deviation shown in table 4-1 for the removed mass measured with the above mentioned techniques. Therefore this change in local glass density explains the deviation of the two aforementioned methods to measure the removed mass.

A possible explanation for the change in density of the machined substrate could be the fact that the substrate is quenched quickly during machining. Decreasing of soda lime glass density by fast cooling has been reported in literature [39]. The local machining temperature is reported to be more than 600°C [4, 29]. The glass surface is locally exposed to the electrochemical discharges for a short period of time and cools quickly when the tool moves away. The temperature on the surface also drops dramatically with distance from the machining tool. As mentioned above, the machining voltage and speed are the same in all experiments. Therefore the exposed energy and the local machining temperature remain constant for all experiments. If all samples are cooled with the same rate, then the change in the density should be equal for all the experiments regardless of the electrolyte concentration. The equal percent deviations obtained in table 4-1 confirm this.

4.3. Etching machined samples with HF

Samples machined with different electrolyte concentrations were dipped inside 20v/v% HF solution for 20 minutes. The micro-channels' surface machined with SACE technique are observed to be etched with lower rate than the unmachined glass surface. This difference in the chemical etching rate can be attributed to the difference in glass properties as discussed in section 4.2. Different groups have reported that fused silica is locally densified when exposed to low energy femtosecond laser pulses and this densification plays the role of a mask to selectively etch glass with HF [40]. Youn *et al.* [41] reported the maskless etching of glass by making nano-scratches on the glass surface based on the same phenomenon. As discussed in section 4.2, the local density of the micro-channels decreases during machining and glass density on micro-channels surface

is lower than for the unmachined surface. The result from the experiments with HF solution confirms the same observation and shows that the low density portion of the glass surface is etched with lower rate by HF.

4.4. Conclusion

In this chapter, 2D-micro-machining with a micro-channel pattern was performed on the soda-lime glass samples by Spark Assisted Chemical Engraving technology. The difference in hardness of the machined areas showed that the material becomes softer after machining. This softening is an indication of changes in glass density. The difference between calculations of removed mass by analytical balance and geometrical methods, followed by the results from the nano-indentation test indicate that the density of the machined surface decreases during the machining process. This change of density is attributed to the fast cooling of the work-piece during machining process. The results were confirmed by the observation that the low density portion of the glass surface inside the micro-channel is etched with a lower rate compared to the unmachined glass surface.

5. Conclusions, Original Contributions to knowledge and Future Prospective

As a result of investigations discussed in previous chapters, fabrication of a combination of micro-channels with through micro-holes as inlet and outlet wells is presented in this chapter. Also, two new techniques, one related to machining and one related to bonding, are proposed to enhance the surface quality in the final device. In addition, a Y shape microfluidic pattern for testing the applicability of surface roughness in micro-mixing is introduced. Finally, a conclusion of the results from previous chapters is presented and some original ideas for future investigations are proposed.

5.1. Simultaneous micro-hole drilling and micro-channel machining

Alignment is a serious issue in the fabrication of devices that require combination of holes and channels with different geometries and coordinates on a surface. Using SACE technology, it is possible to fabricate a combination of micro-holes and micro-channels with desired geometry and quality without changing the electrolyte and tool. Therefore the precision of the coordinates of different patterned components of a device can be controlled. The main advantage of this system is fabrication of all-through micro-holes as inlet and outlets ports of micro-channels.

Figure 5-1 shows a simple microfluidic channel with inlet and outlet, fully fabricated by SACE. The width of the micro-channel is 300 microns with 250 μ m depth. Diameters of the inlet and outlet of the micro-channel are 1mm and the glass sample used is 2mm thick. As shown in figure 5-1, boundaries around the micro-holes are heat affected. This is due to applying high voltage (around 35V). By decreasing the applied voltage and thus the energy exposed to the glass surface it is possible to achieve better surface qualities. Figure 5-2 shows the 3D view of the design for the whole device using MDT software (Autodesk®). The overall capacity of this device is about 7 μ L. The inlet well capacity is approximately 3.2 μ L.

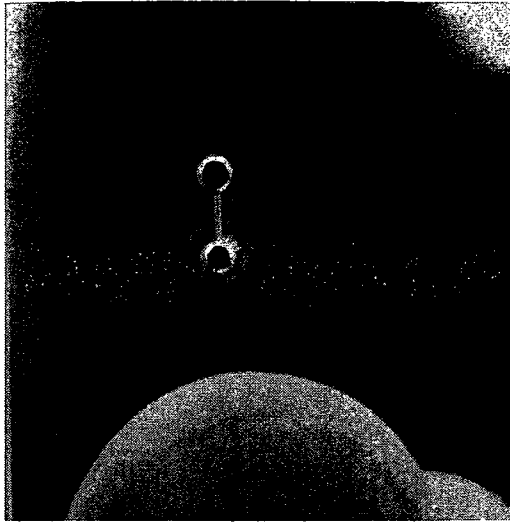


Figure 5-1. Micro-channel with two all-through holes as inlet and outlet

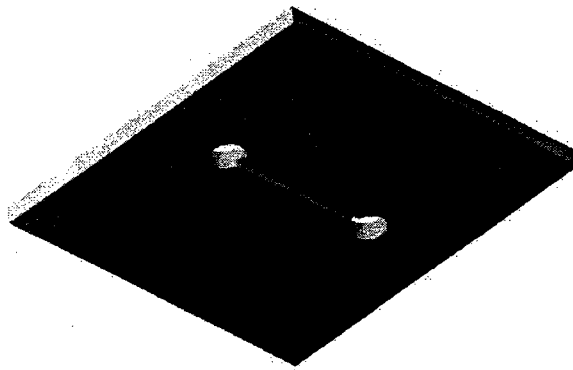


Figure 5-2. 3D view of the design drawing for the simple device by MDT software (Autodesk®)

5.2. Simple techniques to enhance surface quality

Using different machining tool shapes, it is almost possible to achieve any desired geometry of micro-holes and micro-channels. However, it is not always possible to control the quality of the surface of the micro-channel. In addition to applying all the machining parameters and polishing techniques to enhance the quality of the surface, two new techniques, one related to machining and one related to bonding, are proposed to enhance the surface quality.

The first technique, which is related to fabrication, is to use a needle shaped tool for micro-machining. In this technique, first a micro-channel is machined using a typical needle as machining tool. The width of this micro-channel is about 30 microns. Then the tool is moved 30 microns along the width of the micro-channel and the machining process is repeated again. The result is a micro-channel with 60 microns width. By repeating this procedure it is possible to achieve micro-channels with 500 μm width. Repeating the machining without moving the tool along the width will also result in deeper micro-channels. Therefore it is possible to achieve any desired geometry while the surface quality remains acceptable as a result of using needle as the machining tool. The micro-channel in Figure 5-1 has been fabricated using the mentioned technique.

Second technique, related to assembly of the final device, is to use a flat glass surface as another substrate, which has not been machined. The new substrate is used as the bottom surface of the micro-channel in which the fluid moves along. Bonding of two glass substrates is a difficulty which can be solved by heating the substrates up to 700°C and cooling them very slowly.

5.3. Proposal of a new microfluidic device for statistical studies in bio applications

It is also possible to fabricate complex microfluidic devices by SACE. Figure 5-3 shows a new design for bio applications. In this configuration, 16 micro-channels with the same inlet would be used to allow the statistical study of the behavior of the species in the fluid. Micro-channels with decreasing cross sectional area (nozzle shape), can also be fabricated to study capillary effects.

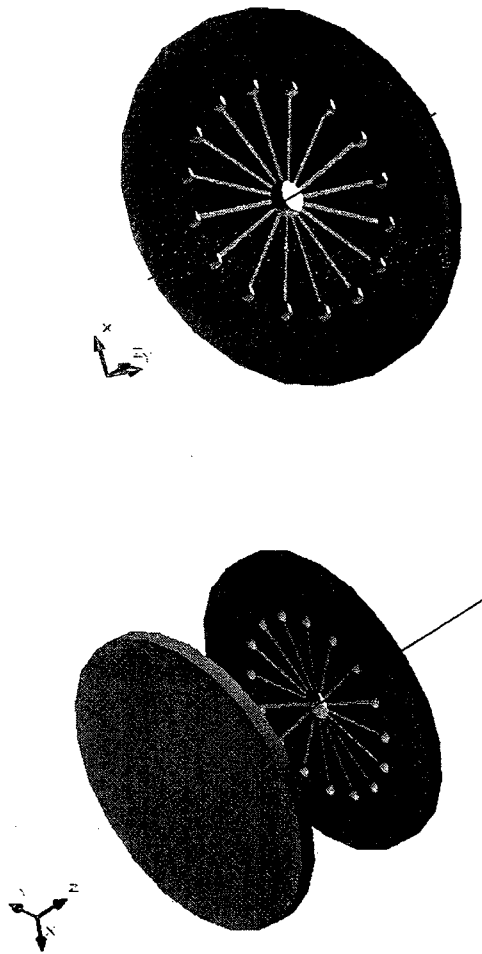


Figure 5-3. 3D-design of a microluidic device for statistical study in bio applications

5.4. Fabrication of micro-mixers based on surface roughness

Figure 5-4 shows a micro-channel machined with 10 %wt NaOH electrolyte. The obtained pattern in this figure shows a micro-channel surface composed of small scratches. This is an interesting observation. Mixing is a challenging issue in microfluidic devices, therefore micro-channels machined with lower electrolyte concentrations, like the one shown in figure 5-4, can be used for fabrication of micro-mixers based on the

roughness of the surface. Figure 5-5 shows a Y shape microfluidic device with inlet and outlet wells fully fabricated by SACE which can be used to test the efficiency of mixing.

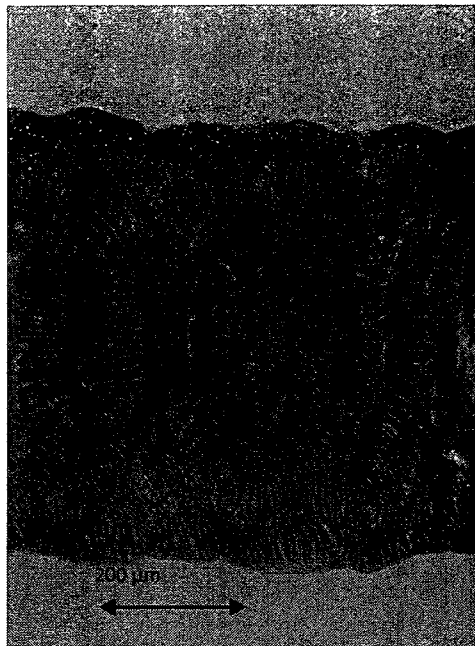


Figure 5-4. Micro-channel machined with 10 %wt NaOH electrolyte

The fabricated patterns using SACE technology can also be used as a mould for batch fabrication in soft lithography.

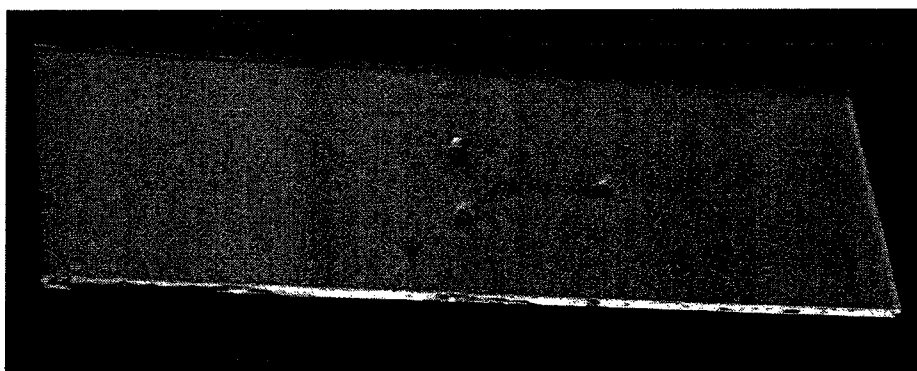


Figure 5-5. Y shape microfluidic device with inlet and outlet wells fabricated by SACE for mixing applications

5.5. Conclusions and original contributions to knowledge

Micro-fabrication is a crucial step in miniaturization of devices, thus it is important to develop novel, trustable and economic technologies for this purpose. Spark Assisted Chemical Engraving (SACE) is an unconventional micro-machining technique which is not only economic for prototype fabrication but can also fabricate high aspect ratio structures without any need for clean room environments. The goal of this study was to develop the SACE technique for 2D-micro-machining and gain a deep understanding of the parameters affecting machining process and final sample quality. The main contributions of this thesis are categorized as follows:

- Establishment of the SACE micro-machining set-up
- Introducing a systematic procedure for 2D-micro-machining with SACE
- Proposing a characterization diagram for fabrication of micro-channels to achieve desired micro-channel quality and geometry
- Chemical contributions to the mechanism of material removal
- Changes in glass properties machined by SACE
- Micro-fluidic devices with through inlet and outlet wells fabricated fully by SACE
- Original ideas for prospective study

It was shown in this thesis that the best micro-channel quality with desired depth can be achieved in voltages less than 32V and tool velocity less than 30 $\mu\text{m/s}$ at tool distance less than 15 μm microns from the glass surface and a qualitative model with achievable geometrical properties of the micro-channels was presented.

Material removal mechanism in SACE micro-machining was investigated through a set of different experiments. Experimental results for removed material and FT-IR analysis on the machined samples together with the results from Inductive Coupled Plasma Mass Spectrometry (ICP-MS) test for the silicon concentration inside electrolyte after machining showed that chemical etching at high local temperatures is the major phenomenon contributing to the machining process.

20% deviation between calculations of removed mass by analytical balance and geometrical methods showed that glass properties change after machining. Performing nano-indentation test on the machined samples confirmed that the hardness and density of the machined surface decrease during the machining process. This change of density is attributed to the fast cooling of the work-piece during machining. The low density portion of the glass surface inside the micro-channel is etched with a lower rate compared to the unmachined glass surface which is another indication of decreasing glass substrates local density after machining.

2D-micro-machining by SACE technology with constant velocity is a new approach for 2D-micro-machining which can be used together with micro-holes drilled with SACE to fabricate a complete microfluidic device. In this thesis a simple micro-channel with inlet and outlet wells and a Y shape microfluidic device, fully fabricated by SACE was introduced. By combining different patterns of micro-holes and micro-channels, any desired geometry is achievable.

5.6. Ideas for future work

To develop SACE for micro-fluidic and Lab-on-a-Chip applications, it is proposed to further investigate the following:

- Enhancing the quality of the machined micro-channels for biomedical applications
- Characterizing the roughness of the machined micro-channels based on the machining parameters and its efficiency as a micro-mixer
- Using glass substrates machined with SACE as moulds for soft lithography
- Deposition of metallic micro and nano particles on glass micro-channels during machining to avoid later conductive layer deposition for electrokinetic applications

References

- [1] G. M. Whitesides, "The origins and the future of microfluidics," *Nature*, vol. 442(7101), pp. 368-373, 2006.
- [2] S. Franssila, *Introduction to micro fabrication*: John Wiley and Sons Ltd, 2004.
- [3] R. Wüthrich and V. Fascio, "Machining of non-conducting materials using electrochemical discharge phenomenon - an overview," *International Journal of Machine Tools & Manufacture*, vol. 45, pp. 1095-1108, Jul 2005.
- [4] T. Fatanat Didar, A. Dolatabadi, and R. Wüthrich, "Characterization and modeling of 2D-glass micro-machining by spark assisted chemical engraving (SACE) with constant velocity," *Accepted to Journal of micromechanics and microengineering*, 2008.
- [5] P. Maillard, B. Despont, H. Bleuler, and R. Wüthrich, "Geometrical characterization of micro-holes drilled in glass by gravity-feed with spark assisted chemical engraving (SACE)," *Journal of micromechanics and microengineering*, vol. 17, pp. 1343-1349, 2007.
- [6] H. Kurafuji and K. Suda, "Electrical discharge drilling of glass," *Ann. CIPR*, vol. 16, pp. 415-9, 1968.
- [7] A. Lal, H. Bleuler, and R. Wüthrich, "Fabrication of metallic nanoparticles by electrochemical discharges," *Electrochemistry Communications*, vol. 10, pp. 488-491, 2008.
- [8] C. Tsutsumi, K. Okano, and T. Suto, "High quality machining of ceramics," *Journal of Materials Processing Technology*, vol. 37, pp. 639-654, Feb 1993.
- [9] Y. P. Singh, V. K. Jain, P. Kumar, and D. C. Agrawal, "Machining piezoelectric (PZT) ceramics using an electrochemical spark machining (ECSM) process," *Journal of Materials Processing Technology*, vol. 58, pp. 24-31, Mar 1996.
- [10] N. H. Cook, G. B. Foote, P. Jordan, and B. N. Kalyani, "Experimental studies in electro-machining," *American Society of Mechanical Engineers (Paper)*, p. 6, 1972.
- [11] R. Wüthrich, U. Spaelter, and H. Bleuler, "The current signal in spark-assisted chemical engraving (SACE): what does it tell us?," *Journal of micromechanics and microengineering*, vol. 16, pp. 779-785, 2005.

- [12]R. Wüthrich and L. A. Hof, "The gas film in spark assisted chemical engraving (SACE) - A key element for micro-machining applications," *International Journal of Machine Tools & Manufacture*, vol. 46, pp. 828-835, Jun 2006.
- [13]R. Wüthrich, U. Spaelter, Y. Wu, and H. Bleuler, "A systematic characterization method for gravity-feed micro-hole drilling in glass with spark assisted chemical engraving (SACE)," *Journal of Micromechanics and Microengineering*, vol. 16, pp. 1891-1896, Sep 2006.
- [14]Z. P. Zheng, H. C. Su, F. Y. Huang, and B. H. Yan, "The tool geometrical shape and pulse-off time of pulse voltage effects in a Pyrex glass electrochemical discharge microdrilling process," *Journal of Micromechanics and Microengineering*, vol. 17, pp. 265-272, Feb 2007.
- [15]V. Fascio, R. Wuthrich, K. Fujisaki, D. Viquerat, H. Langen, and H. Bleuler, "Spark assisted chemical engraving: a novel technology for glass microstructuring (43)," in *Invited lecture in European Congress on Advanced Materials and Processes (EUROMAT) Lausanne*, 2003.
- [16]R. Wüthrich, V. Fascio, D. Viquerat, and H. Langen, "Study of spark assisted chemical engraving-process technology data," in *International Conference of the European Society for Precision Engineering and Nanotechnology (EUSPEN) 1 (31) Eindhoven: 265-268*, 2002.
- [17]R. Wüthrich, "Spark assisted chemical engraving—a stochastic modeling approach," in *Swiss Federal Institute of Technology*. vol. Doctor of Philosophy Lausanne: EPFL, 2003.
- [18]H. Langen, I. Ceausoglu, M. Van der Meer, E. Lehmann, H. Bleuler, and P. Renaud, "Electrochemical micromachining of glass using Mico-EDMed Microtools," in *Proceedings of Ultraprecision in Manufacturing Engineering*, Braunschweig, 1997, p. 672.
- [19]R. Wüthrich, V. Fascio, D. Viquerat, and H. Langen, "In situ measurement and micro-machining of glass " *International Symposium on Micromechatronics and Human Science*, pp. 185-191, 1999.
- [20]V. Fascio, H. H. Langen, H. Bleuler, C. Comminellis, and "Investigations of the spark assisted chemical engraving " *Electrochemistry Communications*, vol. 5, pp. 203-207, 2003.
- [21]Z. Zheng, W. CHENG, F. Huang, and B. Yan, "3D microstructuring of Pyrex glass using the electrochemical discharge machining process," *Journal of micromechanics and microengineering*, vol. 17, pp. 960-966, 2007.

- [22] M. Han, B. Min, and S. Lee, "Improvement of surface integrity of electro-chemical discharge machining process using powder-mixed electrolyte," *Journal of Materials Processing Technology*, vol. 191, pp. 224-227, 2007.
- [23] V. K. Jain, P. S. Rao, S. K. Choudhary, and K. P. Rajurkar, "Experimental investigations into traveling wire electrochemical spark machining (TW-ECSM) of composites," *Journal of Engineering for Industry-Transactions of the Asme*, vol. 113, pp. 75-84, Feb 1991.
- [24] K. Allesu, A. Ghosh, and M. K. Muju, "Preliminary qualitative approach of a proposed mechanism of material removal in electrical machining of glass " *European Journal Mech. Eng.*, vol. 36, p. 202, 1992.
- [25] V. K. Jain, S. K. Choudhury, and K. M. Ramesh, "On the machining of alumina and glass," *International Journal of Machine Tools & Manufacture*, vol. 42, pp. 1269-1276, Sep 2002.
- [26] V. K. Jain and S. K. Chak, "Electrochemical spark trepanning of alumina and quartz," *Machining Science and Technology*, vol. 4, pp. 277-290, 2000.
- [27] N. H. Cook, G. B. Foote, P. Jordan, and B. N. Kalyani, "Experimental studies in electro-machining," *American Society of Mechanical Engineers (Paper)*, p. 6, 1972.
- [28] Y. Liao and W. Peng, "Study of hole-machining on pyrex wafer by electrochemical discharge (ECDM)," *Materials Science Forum*, vol. 505-507, pp. 1207-1212, 2006.
- [29] M. Jalali, P. Maillard, H. Bleuler, and R. Wüthrich, "Towards a better understanding of Glass Gravity-Feed Micro-hole Drilling with Electrochemical Discharges," *Submitted to International Journal of micromechanics and microengineering*.
- [30] V. Fascio, "Etude de la microstructuration du verre par étincelage assisté par attaque chimique : une approche électrochimique," in *Swiss Federal Institute of Technology*. vol. Doctor of Philosophy Lausanne: no 2691 EPFL, 2002.
- [31] C. T. Yang, S. S. Ho, and B. H. Yan, "Micro Hole Machining of Borosilicate Glass through Electrochemical Discharge machining (ECDM)," *Key Engineering Materials*, vol. 196 pp. 149-166, 2001.
- [32] H. Tokura, I. Kondoh, and M. Yoshikawa, "Ceramic material processing by electrical discharge in electrolyte," *Journal of Material Science*, vol. 24, p. 991, 1989.

- [33] V. K. Jain and S. Adhikary, "On the mechanism of material removal in electrochemical spark machining of quartz under different polarity conditions," *Journal of materials processing technology*, vol. 200, pp. 460-470
2008.
- [34] J. West and A. Jadhav, "ECDM methods for fluidic interfacing through thin glass substrates and the formation of spherical microcavities," *Journal of Micromechanics and Microengineering*, vol. 17, pp. 403-409, 2007.
- [35] A. Hickling and M. D. Ingram, "Glow discharge electrolysis," *Journal of electroanalytical chemistry*, vol. 8, p. 65, 1964.
- [36] P. Maillard, "Investigation on material removal process in SACE glass machining - Design of a force measuring set-up." vol. Master of Science Lausanne: Ecole Polytechnique de Lausanne (EPFL), 2007.
- [37] R. Wüthrich, L. A. Hof, L. Lal, K. Fujisaki, H. Bleuler, P. Mandin, and G. Picard, "Physical principles and miniaturization of Spark Assisted Chemical Engraving (SACE)," *Journal of Micromechanics and Microengineering*, pp. 268-275, 2005
- [38] N. P. e. a. Bansal, *Handbook of glass properties*. Orlando: Academic press, 1986.
- [39] J. E. Shelby, *Introduction to glass science and technology*. Cambridge Royal Science of Chemistry, 1997.
- [40] Y. Bellouard, M. Dugan, A. A. Said, and P. Bado, "Thermal conductivity contrast measurement of fused silica exposed to low-energy femtosecond laser pulses," *Applied Physics Letters*, vol. 89, 2006.
- [41] S. W. Youn and C. G. Kang, "Maskless pattern fabrication on Pyrex 7740 glass surface by using nano-scratch with HF wet etching," *Scripta Materialia* vol. 52, pp. 117-122, 2005.

Appendix

Examples of computer codes developed for micro-machining with TCL scripting language

1- Computer code for touching the glass surface:

This procedure detects the samples surface and reports its coordinate on the screen

```
proc FindZero {socketID Z} {

    upvar $Z Zfinal

    puts stdout "Searching for the glass surface"

    # Change velocity to slow one
    set code [catch "PositionerSGammaParametersSet $socketID XYZ.Z 0.2 400 0.001 0.001"]
    if {$code != 0} {
        DisplayErrorAndClose $socketID $code "PositionerSGammaParametersSet"
        return
    }

    # Configure Event
    set code [catch "EventExtendedConfigurationTriggerSet $socketID
GPIO2.ADC1.ADCLowLimit 5.2 0 0 0 XYZ.Z.SGamma.MotionState 0 0 0 0"]
    if {$code != 0} {
        DisplayErrorAndClose $socketID $code "EventExtendedConfigurationTriggerSet"
        return
    }

    set code [catch "EventExtendedConfigurationActionSet $socketID XYZ.MoveAbort 0 0 0 0" ]
    if {$code != 0} {
        DisplayErrorAndClose $socketID $code "EventExtendedConfigurationActionSet"
        return
    }

    # Start event
    set code [catch "EventExtendedStart $socketID EvID"]
    if {$code != 0} {
        DisplayErrorAndClose $socketID $code "EventExtendedStart"
        return
    }

    # Start motion to touch the glass surface
    set code [catch "GroupMoveRelative $socketID XYZ.Z 10"]
    if {$code != 0} {
        if {$code == -27} {
            puts stdout "Glass surface detected"
        } else {
            puts stdout "ERROR Glass surface not detected"
            DisplayErrorAndClose $socketID $code "FindZero"
        }
    }
}
```

```

        return -1
    }
}

# gets the position
set code [catch "GroupPositionCurrentGet $socketID XYZ.Z Zfinal"]
if {$code != 0} {
    DisplayErrorAndClose $socketID $code "GroupPositionCurrentGet"
    return
}

set code [catch "EventExtendedRemove $socketID $EvID"]
if {$code != 0} {
    DisplayErrorAndClose $socketID $code "EventExtendedRemove"
    return
}

puts stdout "glass surface detected at Z=$Zfinal"
}

```

2- Computer code for 2D-micro-machining

This code is for fabricating series of micro-channels on a substrate with subsequent depth measurement

```

#Display error and close procedure
proc DisplayErrorAndClose {socketID code APIName} {
    global tcl_argv
    if {$code != -2 && $code != -108} {
        set code2 [catch "ErrorStringGet $socketID $code strError"]
        if {$code2 != 0} {
            puts stdout "$APIName ERROR => $code - ErrorStringGet ERROR
=> $code2"

            set tcl_argv(0) "$APIName ERROR => $code"
        } else {
            puts stdout "$APIName $strError"
            set tcl_argv(0) "$APIName $strError"
        }
    } else {
        if {$code == -2} {
            puts stdout "$APIName ERROR => $code : TCP timeout"
            set tcl_argv(0) "$APIName ERROR => $code : TCP timeout"
        }
        if {$code == -108} {
            puts stdout "$APIName ERROR => $code : The TCP/IP connection
was closed by an administrator"
            set tcl_argv(0) "$APIName ERROR => $code : The TCP/IP
connection was closed by an administrator"
        }
    }
}

```

```

        set code2 [catch "TCP_CloseSocket $socketID"]
        return
    }

    #Main process
    set TimeOut 7000
    set code 0
    set p 1

    #machinging Speed
    set s 2

    # Voltage
    set v 2.05128

    #Distance from glass while machining

    puts stdout "*****"

    puts stdout ">>> Starting 2D machining process"

    puts stdout "Machinning speed is $s mm per second"

    set voltage [expr { 15.6 * $v}]

    puts stdout "Applied Voltage is $voltage V"

    # load the FindZero function
    source //Admin//Public//Scripts//FindZero.tcl

    #Open TCP socket
    OpenConnection $TimeOut socketID
    if {$socketID == -1} {
        puts stdout "OpenConnection failed => $socketID"
        return
    }

    #####
    # Move Z`axis down

    puts stdout "Move Z axis down to start..."

    set code [catch "PositionerSGammaParametersSet $socketID XYZ.Z 2 400 0.001 0.001"]
    if {$code != 0} {
        DisplayErrorAndClose $socketID $code "PositionerSGammaParametersSet"
        return
    }

    set code [catch "GroupMoveRelative $socketID XYZ.Z 8"]
    if {$code != 0} {

```

```

        DisplayErrorAndClose $socketID $code "GroupMoveRelative"
    return
}

set code [catch "PositionerSGammaParametersSet $socketID XYZ.X 2 400 0.001 0.001"]
    if {$code != 0} {
        DisplayErrorAndClose $socketID $code "PositionerSGammaParametersSet"
    return
}

    set code [catch "GroupMoveRelative $socketID XYZ.X -25"]
    if {$code != 0} {
        DisplayErrorAndClose $socketID $code "GroupMoveRelative"
    return
}

set code [catch "PositionerSGammaParametersSet $socketID XYZ.Y 2 400 0.001 0.001"]
    if {$code != 0} {
        DisplayErrorAndClose $socketID $code "PositionerSGammaParametersSet"
    return
}

    set code [catch "GroupMoveRelative $socketID XYZ.Y 10"]
    if {$code != 0} {
        DisplayErrorAndClose $socketID $code "GroupMoveRelative"
    return
}
}
#####
# Start the For Loop

for {set i 1} {$i<3} {incr i} {

    puts stdout "#####"

    puts stdout "Starting Fabrication of the $i th Channel"

    set p [expr {100 * $i}]

    set path //Admin//Public//$p

    set q [open $path "a+"]

    #####
    # Finds the first point

    puts stdout ">>>> Finding the first point of the $i th channel"

    FindZero $socketID Z

    puts stdout ">>>> Z = $Z"

    set Z1 $Z

    puts $q "Z1=$Z"

    set p1 [expr {-1 * $Z1}]
}

```

```

#####
# Move up the Z axis

    puts stdout "Moving Z axis up"

    set code [catch "PositionerSGammaParametersSet $socketID XYZ.Z 1 400
0.001 0.001"]
    if {$code != 0} {
        DisplayErrorAndClose          $socketID          $code
"PositionerSGammaParametersSet"
        return
    }

    set code [catch "GroupMoveRelative $socketID XYZ.Z -2"]
    if {$code != 0} {
        DisplayErrorAndClose $socketID $code "GroupMoveRelative"
    }
    return
}
#####
# Move the X axis to find the second point of channel

    puts stdout "Moving X axis"

    set code [catch "PositionerSGammaParametersSet $socketID XYZ.X 2 400
0.001 0.001"]
    if {$code != 0} {
        DisplayErrorAndClose          $socketID          $code
"PositionerSGammaParametersSet"
        return
    }

    set code [catch "GroupMoveRelative $socketID XYZ.X 15"]
    if {$code != 0} {
        DisplayErrorAndClose $socketID $code "GroupMoveRelative"
    }
    return
}
#####
# Finds the second point of channel

    puts stdout ">>>> Finding the second point of the $i th channel"

    FindZero $socketID Z

    puts stdout ">>>> Z2 = $Z"

    set Z2 $Z

    set DZ [expr {$Z1 - $Z2}]

    puts $q "Z2=$Z"

    set p2 [expr {-1 * $Z2}]

    set d [expr {$p1 - $p2}]

```

```

set a [expr {$d / 15}]

#set b [expr {-1 * $Z2}]

puts $q "The Chaneel line equation: z= $a x"
#####3
# Go up 5 microns plus 0.07

puts stdout "Move Z axis up to start..."

set code [catch "PositionerSGammaParametersSet $socketID XYZ.Z 0.1 400 0.001
0.001"]
if {$code != 0} {
    DisplayErrorAndClose $socketID $code "PositionerSGammaParametersSet"
return
}

set code [catch "GroupMoveRelative $socketID XYZ.Z -0.06"]
if {$code != 0} {
    DisplayErrorAndClose $socketID $code "GroupMoveRelative"
return
}

#####
# Doing the microchannel fabrication and gathering data

set code [catch "PositionerSGammaParametersSet $socketID XYZ.Z $s 400
0.001 0.001"]
if {$code != 0} {
    DisplayErrorAndClose $socketID $code
"PositionerSGammaParametersSet"
return
}

set code [catch "PositionerSGammaParametersSet $socketID XYZ.X $s 400
0.001 0.001"]
if {$code != 0} {
    DisplayErrorAndClose $socketID $code
"PositionerSGammaParametersSet"
return
}

#####
# Turn on the power

set code [catch "GPIOAnalogSet $socketID GPIO2.DAC4 $v"]
if {$code != 0} {
    DisplayErrorAndClose $socketID $code "GPIOAnalogSet"
return
}

puts stdout "Electrodischarge starts for 2D machining..."

```

```

        set code [catch "GatheringConfigurationSet $socketID XYZ.Z.CurrentPosition
GPIO2.ADC1 GPIO2.ADC2"]
        if {$code != 0} {
            DisplayErrorAndClose $socketID $code "GatheringConfigurationSet"
        }
        return
    }

    set code [catch "EventExtendedConfigurationTriggerSet $socketID
XYZ.Z.SGamma.MotionState 0 0 0 0"]
    if {$code != 0} {
        DisplayErrorAndClose $socketID $code
        "EventExtendedConfigurationTriggerSet"
    }
    return
}

set code [catch "EventExtendedConfigurationActionSet $socketID
GatheringRun 33333 3 0 0"]
if {$code != 0} {
    DisplayErrorAndClose $socketID $code
    "EventExtendedConfigurationActionSet"
}
return
}

set code [catch "EventExtendedStart $socketID arg1"]
if {$code != 0} {
    DisplayErrorAndClose $socketID $code "EventExtendedStart"
}
return
}

set code [catch "GroupMoveRelative $socketID XYZ -15,0,$DZ"]
if {$code != 0} {
    DisplayErrorAndClose $socketID $code "GroupMoveRelative"
}
return
}

set code [catch "GatheringStopAndSave $socketID "]
if {$code != 0} {
    DisplayErrorAndClose $socketID $code "GatheringStopAndSave"
}
return
}

#Change the gathered file name

set new_name //Admin//Public//$i
puts stdout "$new_name"
file rename -force -- //Admin//Public//Gathering.dat $new_name

# Stop the discharge

set code [catch "GPIOAnalogSet $socketID GPIO2.DAC4 0"]
if {$code != 0} {
    DisplayErrorAndClose $socketID $code "GPIOAnalogSet"
}
return
}

```



```

puts stdout "Electrodischarge stops"

#####
#Move up the Z axis

set code [catch "PositionerSGammaParametersSet $socketID XYZ.Z 2 400
0.001 0.001"]
if {$code != 0} {
    DisplayErrorAndClose $socketID $code
"PositionerSGammaParametersSet"
return
}
set code [catch "GroupMoveRelative $socketID XYZ.Z -2"]
if {$code != 0} {
    DisplayErrorAndClose $socketID $code "GroupMoveRelative"
return
}

puts stdout "The $i th channel is finished"

# Measure the depth

puts stdout "Procedure for measuring the depth starts"

set code [catch "PositionerSGammaParametersSet $socketID XYZ.X 2 400
0.001 0.001"]
if {$code != 0} {
    DisplayErrorAndClose $socketID $code
"PositionerSGammaParametersSet"
return
}

set code [catch "GroupMoveRelative $socketID XYZ.X 12"]
if {$code != 0} {
    DisplayErrorAndClose $socketID $code "GroupMoveRelative"
return
}

#####
# measure the depth of channel

set m 3

set sum 0

for {set k 10} {$k < 20} {incr k} {

    FindZero $socketID Z

    set pd [expr {-1 * $Z}]

    #set code [catch "GroupPositionCurrentGet $socketID XYZ.Z Depth"]
    #if {$code != 0} {

```

```

#      DisplayErrorAndClose      $socketID      $code
"GroupPositionCurrentGet"
#return
#}
#####
#Calculate the depth

puts stdout "Calculating the depth of the $k point"

set SurfaceBeforeDrilling [expr {$a * $m}]

set pf [expr {$pd - $p2}]

set Depth [expr {$SurfaceBeforeDrilling - $pf}]

puts stdout "$k th Depth = $Depth"

set sum [expr {$sum + $Depth}]

puts stdout "sum= $sum"

puts $q "$k Depth= $Depth"

#####
# move axis to find the next depth

set code [catch "PositionerSGammaParametersSet $socketID XYZ.Z 2
400 0.001 0.001"]
if {$code != 0} {
    DisplayErrorAndClose      $socketID      $code
"PositionerSGammaParametersSet"
return
}

set code [catch "GroupMoveRelative $socketID XYZ.Z -1"]
if {$code != 0} {
    DisplayErrorAndClose      $socketID      $code
"GroupMoveRelative"
return
}

set code [catch "PositionerSGammaParametersSet $socketID XYZ.X 1
400 0.001 0.001"]
if {$code != 0} {
    DisplayErrorAndClose      $socketID      $code
"PositionerSGammaParametersSet"
return
}

set code [catch "GroupMoveRelative $socketID XYZ.X -1"]
if {$code != 0} {
    DisplayErrorAndClose      $socketID      $code
"GroupMoveRelative"
return
}

```

```

set m [expr {$m + 1}]

}

# find the average channel depth

set AverageDepth [expr {$sum / 10}]

puts stdout "The average depth for the $i channel is = $AverageDepth"

puts $q "Average channel depth for channel $i is = $AverageDepth"

#Take the position to start the next channel

set code [catch "PositionerSGammaParametersSet $socketID XYZ.X 2 400 0.001 0.001"]
if {$code != 0} {
    DisplayErrorAndClose $socketID $code "PositionerSGammaParametersSet"
    return
}

set code [catch "GroupMoveRelative $socketID XYZ.X -2"]
if {$code != 0} {
    DisplayErrorAndClose $socketID $code "GroupMoveRelative"
}
return

}

#####
#Move Y axis left for the next channel

puts stdout "Move Y axis to fabricate the next channel"

set code [catch "PositionerSGammaParametersSet $socketID XYZ.Y 1 400
0.001 0.001"]
if {$code != 0} {
    DisplayErrorAndClose $socketID $code
"PositionerSGammaParametersSet"
    return
}

set code [catch "GroupMoveRelative $socketID XYZ.Y 3"]
if {$code != 0} {
    DisplayErrorAndClose $socketID $code "GroupMoveRelative"
}
return
}
close $q

set code [catch "GatheringReset $socketID "]
if {$code != 0} {
    DisplayErrorAndClose $socketID $code "GatheringReset"
}
return

}
}

```

```

#####
puts stdout ">>>> 2D micro-machining for the first 5 channel series, has been successfully
finished"

#####
#####
# Start machining of the second 6 channel series
puts                                     stdout
"_____ "

# Move X and Y Axis to start the second 6 channel series

set code [catch "PositionerSGammaParametersSet $socketID XYZ.X 2 400 0.001 0.001"]
    if {$code != 0} {
        DisplayErrorAndClose $socketID $code "PositionerSGammaParametersSet"
    }
    return
}

set code [catch "GroupMoveRelative $socketID XYZ.X 20"]
    if {$code != 0} {
        DisplayErrorAndClose $socketID $code "GroupMoveRelative"
    }
    return
}

set code [catch "PositionerSGammaParametersSet $socketID XYZ.Y 1 400 0.001 0.001"]
    if {$code != 0} {
        DisplayErrorAndClose $socketID $code "PositionerSGammaParametersSet"
    }
    return
}

set code [catch "GroupMoveRelative $socketID XYZ.Y -6"]
    if {$code != 0} {
        DisplayErrorAndClose $socketID $code "GroupMoveRelative"
    }
    return
}

# Start the For Loop

for {set i 3} {$i<6} {incr i} {

    puts stdout "#####"

    puts stdout "Starting Fabrication of the $i th Channel"

    set p [expr {100 * $i}]

    set path //Admin//Public//$p

    set q [open $path "a+"]

    #####
    # Finds the first point

```

```

puts stdout ">>> Finding the first point of the $i th channel"

FindZero $socketID Z

puts stdout ">>>> Z = $Z"

set Z1 $Z

puts $q "Z1=$Z"

set p1 [expr {-1 * $Z1}]

#####
# Move up the Z axis

        puts stdout "Moving Z axis up"

        set code [catch "PositionerSGammaParametersSet $socketID XYZ.Z 1 400
0.001 0.001"]
        if {$code != 0} {
                DisplayErrorAndClose                $socketID                $code
"PositionerSGammaParametersSet"
                return
        }

        set code [catch "GroupMoveRelative $socketID XYZ.Z -2"]
        if {$code != 0} {
                DisplayErrorAndClose $socketID $code "GroupMoveRelative"
                return
        }
#####
# Move the X axis to find the second point of channel

        puts stdout "Moving X axis"

        set code [catch "PositionerSGammaParametersSet $socketID XYZ.X 2 400
0.001 0.001"]
        if {$code != 0} {
                DisplayErrorAndClose                $socketID                $code
"PositionerSGammaParametersSet"
                return
        }

        set code [catch "GroupMoveRelative $socketID XYZ.X 15"]
        if {$code != 0} {
                DisplayErrorAndClose $socketID $code "GroupMoveRelative"
                return
        }
#####
# Finds the second point of channel

        puts stdout ">>> Finding the second point of the $i th channel"

FindZero $socketID Z

```

```

puts stdout ">>>> Z2 = $Z"

set Z2 $Z

set DZ [expr {$Z1 - $Z2}]

puts $q "Z2=$Z"

set p2 [expr {-1 * $Z2}]

set d [expr {$p1 - $p2}]

set a [expr {$d / 15}]

#set b [expr {-1 * $Z2}]

puts $q "The Chaneel line equation: z= $a x"
#####3
# Go up 5 microns plus 0.07

puts stdout "Move Z axis up to start..."

set code [catch "PositionerSGammaParametersSet $socketID XYZ.Z 0.1 400 0.001
0.001"]
if {$code != 0} {
    DisplayErrorAndClose $socketID $code "PositionerSGammaParametersSet"
return
}

set code [catch "GroupMoveRelative $socketID XYZ.Z -0.06"]
if {$code != 0} {
    DisplayErrorAndClose $socketID $code "GroupMoveRelative"
return
}

#####
# Doing the microchannel fabrication and gathering data

set code [catch "PositionerSGammaParametersSet $socketID XYZ.Z $s 400
0.001 0.001"]
if {$code != 0} {
    DisplayErrorAndClose $socketID $code
"PositionerSGammaParametersSet"
return
}

set code [catch "PositionerSGammaParametersSet $socketID XYZ.X $s 400
0.001 0.001"]
if {$code != 0} {
    DisplayErrorAndClose $socketID $code
"PositionerSGammaParametersSet"
return
}

#####

```

```

# Turn on the power

set code [catch "GPIOAnalogSet $socketID GPIO2.DAC4 $v"]
if {$code != 0} {
    DisplayErrorAndClose $socketID $code "GPIOAnalogSet"
return
}

puts stdout "Electrodischarge starts for 2D machining..."

set code [catch "GatheringConfigurationSet $socketID XYZ.Z.CurrentPosition
GPIO2.ADC1 GPIO2.ADC2"]
if {$code != 0} {
    DisplayErrorAndClose $socketID $code "GatheringConfigurationSet"
return
}

set code [catch "EventExtendedConfigurationTriggerSet $socketID
XYZ.Z.SGamma.MotionState 0 0 0 0"]
if {$code != 0} {
    DisplayErrorAndClose $socketID $code
"EventExtendedConfigurationTriggerSet"
return
}

set code [catch "EventExtendedConfigurationActionSet $socketID
GatheringRun 33333 3 0 0"]
if {$code != 0} {
    DisplayErrorAndClose $socketID $code
"EventExtendedConfigurationActionSet"
return
}

set code [catch "EventExtendedStart $socketID arg1"]
if {$code != 0} {
    DisplayErrorAndClose $socketID $code "EventExtendedStart"
return
}

set code [catch "GroupMoveRelative $socketID XYZ -15,0,$DZ"]
if {$code != 0} {
    DisplayErrorAndClose $socketID $code "GroupMoveRelative"
return
}

set code [catch "GatheringStopAndSave $socketID "]
if {$code != 0} {
    DisplayErrorAndClose $socketID $code "GatheringStopAndSave"
return
}

#Change the gathered file name

set new_name //Admin//Public//$i
puts stdout "$new_name"
file rename -force -- //Admin//Public//Gathering.dat $new_name

```

```

# Stop the discharge

set code [catch "GPIOAnalogSet $socketID GPIO2.DAC4 0"]
if {$code != 0} {
    DisplayErrorAndClose $socketID $code "GPIOAnalogSet"
return
}

puts stdout "Electrodischarge stops"

#####
#Move up the Z axis

set code [catch "PositionerSGammaParametersSet $socketID XYZ.Z 2 400
0.001 0.001"]
if {$code != 0} {
    DisplayErrorAndClose $socketID $code
"PositionerSGammaParametersSet"
return
}

set code [catch "GroupMoveRelative $socketID XYZ.Z -1"]
if {$code != 0} {
    DisplayErrorAndClose $socketID $code "GroupMoveRelative"
return
}

puts stdout "The $i th channel is finished"

# Measure the depth

puts stdout "Procedure for measuring the depth starts"

set code [catch "PositionerSGammaParametersSet $socketID XYZ.X 2 400
0.001 0.001"]
if {$code != 0} {
    DisplayErrorAndClose $socketID $code
"PositionerSGammaParametersSet"
return
}

set code [catch "GroupMoveRelative $socketID XYZ.X 12"]
if {$code != 0} {
    DisplayErrorAndClose $socketID $code "GroupMoveRelative"
return
}

#####
# measure the depth of channel

set m 3

set sum 0

```



```

for {set k 10} {$k < 20} {incr k} {

    FindZero $socketID Z

    set pd [expr {-1 * $Z}]

    #set code [catch "GroupPositionCurrentGet $socketID XYZ.Z Depth"]
    #if {$code != 0} {
    #    DisplayErrorAndClose          $socketID          $code
"GroupPositionCurrentGet"
    #return
    #}
    #####
    #Calculate the depth

    puts stdout "Calculating the depth of the $k point"

    set SurfaceBeforeDrilling [expr {$a * $m}]

    set pf [expr {$pd - $p2}]

    set Depth [expr {$SurfaceBeforeDrilling - $pf}]

    puts stdout "$k th Depth = $Depth"

    set sum [expr {$sum + $Depth}]

    puts stdout "sum= $sum"

    puts $q "$k Depth= $Depth"

    #####
    # move axis to find the next depth

    set code [catch "PositionerSGammaParametersSet $socketID XYZ.Z 2
400 0.001 0.001"]
    if {$code != 0} {
        DisplayErrorAndClose          $socketID          $code
"PositionerSGammaParametersSet"
        return
    }

    set code [catch "GroupMoveRelative $socketID XYZ.Z -2"]
    if {$code != 0} {
        DisplayErrorAndClose          $socketID          $code
"GroupMoveRelative"
        return
    }

    set code [catch "PositionerSGammaParametersSet $socketID XYZ.X 1
400 0.001 0.001"]
    if {$code != 0} {
        DisplayErrorAndClose          $socketID          $code
"PositionerSGammaParametersSet"
        return
    }
}

```

```

    }

    set code [catch "GroupMoveRelative $socketID XYZ.X -1"]
    if {$code != 0} {
        DisplayErrorAndClose $socketID $code
    }
}

"GroupMoveRelative"
return
}

set m [expr {$m + 1}]

}

# find the average channel depth
set AverageDepth [expr {$sum / 10}]
puts stdout "The average depth for the $i channel is = $AverageDepth"
puts $q "Average channel depth for channel $i is = $AverageDepth"

#Take the position to start the next channel

set code [catch "PositionerSGammaParametersSet $socketID XYZ.X 2 400 0.001 0.001"]
if {$code != 0} {
    DisplayErrorAndClose $socketID $code "PositionerSGammaParametersSet"
    return
}

set code [catch "GroupMoveRelative $socketID XYZ.X -2"]
if {$code != 0} {
    DisplayErrorAndClose $socketID $code "GroupMoveRelative"
    return
}

#####
#Move Y axis left for the next channel

puts stdout "Move Y axis to fabricate the next channel"

set code [catch "PositionerSGammaParametersSet $socketID XYZ.Y 1 400
0.001 0.001"]
if {$code != 0} {
    DisplayErrorAndClose $socketID $code
}
"PositionerSGammaParametersSet"
return
}

set code [catch "GroupMoveRelative $socketID XYZ.Y 3"]
if {$code != 0} {
    DisplayErrorAndClose $socketID $code "GroupMoveRelative"
}
return
}

```

```

        close $q
        set code [catch "GatheringReset $socketID "]
        if {$code != 0} {
            DisplayErrorAndClose $socketID $code "GatheringReset"
        }
        return
    }
}

puts stdout "*****"
puts stdout "*****"
puts stdout "The hole process for fabrication of 10 channels has been successfully finished"
puts stdout "!!PLEASE DO NOT FORGET TO REMOVE THE GATHERED DATA FROM PUBLIC FOLDER OF XPS!"

# Close TCP socket
TCP_CloseSocket $socketID

```

1- Computer code fabricating the Y shape device

This code is for fabrication of the Y shape device with three through holes as inlets and outlet wells shown in figure 5-5

```

#Display error and close procedure
proc DisplayErrorAndClose {socketID code APIName} {
    global tcl_argv
    if {$code != -2 && $code != -108} {
        set code2 [catch "ErrorStringGet $socketID $code strError"]
        if {$code2 != 0} {
            puts stdout "$APIName ERROR => $code - ErrorStringGet ERROR"
            => $code2"
            set tcl_argv(0) "$APIName ERROR => $code"
        } else {
            puts stdout "$APIName $strError"
            set tcl_argv(0) "$APIName $strError"
        }
    } else {
        if {$code == -2} {
            puts stdout "$APIName ERROR => $code : TCP timeout"
            set tcl_argv(0) "$APIName ERROR => $code : TCP timeout"
        }
        if {$code == -108} {
            puts stdout "$APIName ERROR => $code : The TCP/IP connection
was closed by an administrator"
            set tcl_argv(0) "$APIName ERROR => $code : The TCP/IP
connection was closed by an administrator"
        }
    }
}

```

```

    }
    }
    set code2 [catch "TCP_CloseSocket $socketID"]
    return
}

#Main process
set TimeOut 9000
set code 0
set t 100000

#machining Speed
set s 0.01

# Voltage
set v 1.8
set m 2.11

#Distance from glass while machining

puts stdout "*****"

puts stdout ">>> Starting 2D machining process"

puts stdout "Machining speed is $s mm per second"

set voltage [expr { 15.6 * $v}]

puts stdout "Applied Voltage is $voltage V"

# load the FindZero function
source //Admin//Public//Scripts//FindZero.tcl

#Open TCP socket
OpenConnection $TimeOut socketID
if {$socketID == -1} {
    puts stdout "OpenConnection failed => $socketID"
    return
}

#####
# Move Z axis down

puts stdout "Move Z axis down to start..."

set code [catch "PositionerSGammaParametersSet $socketID XYZ.Z 2 400 0.001 0.001"]
if {$code != 0} {
    DisplayErrorAndClose $socketID $code "PositionerSGammaParametersSet"
    return
}

set code [catch "GroupMoveRelative $socketID XYZ.Z 1"]
if {$code != 0} {

```

```

        DisplayErrorAndClose $socketID $code "GroupMoveRelative"
    return
}

set code [catch "PositionerSGammaParametersSet $socketID XYZ.X 2 400 0.001 0.001"]
if {$code != 0} {
    DisplayErrorAndClose $socketID $code "PositionerSGammaParametersSet"
return
}

set code [catch "GroupMoveRelative $socketID XYZ.X -25"]
if {$code != 0} {
    DisplayErrorAndClose $socketID $code "GroupMoveRelative"
return
}

set code [catch "PositionerSGammaParametersSet $socketID XYZ.Y 2 400 0.001 0.001"]
if {$code != 0} {
    DisplayErrorAndClose $socketID $code "PositionerSGammaParametersSet"
return
}

set code [catch "GroupMoveRelative $socketID XYZ.Y 15"]
if {$code != 0} {
    DisplayErrorAndClose $socketID $code "GroupMoveRelative"
return
}
}
#####
# Start the For Loop

#for {set i 1} {$i<2} {incr i} {

    puts stdout "#####"

    puts stdout "Starting Fabrication of the MicroMixer"

    #####
    # Finds the first point

    puts stdout ">>>> Finding the first point of the MicroMixer"

    FindZero $socketID Z

    puts stdout ">>>> Z3 = $Z"

    set Z3 $Z

    #####
    # Move up the Z axis

        puts stdout "Moving Z axis up"

        set code [catch "PositionerSGammaParametersSet $socketID XYZ.Z 1 400
0.001 0.001"]
        if {$code != 0} {

```

```

                                DisplayErrorAndClose          $socketID          $code
"PositionerSGammaParametersSet"
    return
}

    set code [catch "GroupMoveRelative $socketID XYZ.Z -2"]
    if {$code != 0} {
        DisplayErrorAndClose $socketID $code "GroupMoveRelative"
    }
    return
}
#####
# Move the X axis to find the second point of channel

    puts stdout "Moving X axis"

    set code [catch "PositionerSGammaParametersSet $socketID XYZ.X 2 400
0.001 0.001"]
    if {$code != 0} {
        DisplayErrorAndClose          $socketID          $code
"PositionerSGammaParametersSet"
    }
    return
}

    set code [catch "GroupMoveRelative $socketID XYZ.X 10"]
    if {$code != 0} {
        DisplayErrorAndClose $socketID $code "GroupMoveRelative"
    }
    return
}
#####
# Finds the second point of channel

    puts stdout ">>>> Finding the second point of the channel"

    FindZero $socketID Z

    puts stdout ">>>> Z2 = $Z"

    set Z2 $Z

#####
# Find the first point of the channel for the first fluid

    puts stdout "Moving Z axis up"

    set code [catch "PositionerSGammaParametersSet $socketID XYZ.Z 2 400
0.001 0.001"]
    if {$code != 0} {
        DisplayErrorAndClose          $socketID          $code
"PositionerSGammaParametersSet"
    }
    return
}

    set code [catch "GroupMoveRelative $socketID XYZ.Z -2"]
    if {$code != 0} {
        DisplayErrorAndClose $socketID $code "GroupMoveRelative"
    }
}

```

```

        return
    }

    set code [catch "PositionerSGammaParametersSet $socketID XYZ.X 2 400 0.001 0.001"]
        if {$code != 0} {
            DisplayErrorAndClose $socketID $code
        }
    "PositionerSGammaParametersSet"
    return
}

set code [catch "PositionerSGammaParametersSet $socketID XYZ.Y 2 400 0.001 0.001"]
    if {$code != 0} {
        DisplayErrorAndClose $socketID $code
    }
"PositionerSGammaParametersSet"
return
}

set code [catch "GroupMoveRelative $socketID XYZ 3.5,-3.5,0"]
    if {$code != 0} {
        DisplayErrorAndClose $socketID $code "GroupMoveRelative"
    }
return
}

FindZero $socketID Z

puts stdout ">>>> Z1 = $Z"

set Z1 $Z

set AZ [expr {$Z2 - $Z1}]
set BZ [expr {$Z3 - $Z2}]

#####3
# Go up 5 microns plus 0.07

puts stdout "Move Z axis up to start..."

set code [catch "PositionerSGammaParametersSet $socketID XYZ.Z 0.1 400 0.001
0.001"]
    if {$code != 0} {
        DisplayErrorAndClose $socketID $code "PositionerSGammaParametersSet"
    }
return
}

set code [catch "GroupMoveRelative $socketID XYZ.Z -0.04"]
    if {$code != 0} {
        DisplayErrorAndClose $socketID $code "GroupMoveRelative"
    }
return
}

#####
# Doing the microchannel fabrication for the first fluid channel

set code [catch "PositionerSGammaParametersSet $socketID XYZ.Z $s 400 0.001
0.001"]
    if {$code != 0} {

```

```

                                DisplayErrorAndClose          $socketID          $code
"PositionerSGammaParametersSet"
    return
}

set code [catch "PositionerSGammaParametersSet $socketID XYZ.X $s 400
0.001 0.001"]
if {$code != 0} {
    DisplayErrorAndClose          $socketID          $code
"PositionerSGammaParametersSet"
    return
}

set code [catch "PositionerSGammaParametersSet $socketID XYZ.Y $s 400 0.001
0.001"]
if {$code != 0} {
    DisplayErrorAndClose          $socketID          $code
"PositionerSGammaParametersSet"
    return
}

#####
# Turn on the power

set code [catch "GPIOAnalogSet $socketID GPIO2.DAC1 $v"]
if {$code != 0} {
    DisplayErrorAndClose $socketID $code "GPIOAnalogSet"
return
}

puts stdout "Electrodischarge starts for 2D machining..."

set code [catch "GroupMoveRelative $socketID XYZ -3.5,3.5,$AZ"]
if {$code != 0} {
    DisplayErrorAndClose $socketID $code "GroupMoveRelative"
return
}

set code [catch "GroupMoveRelative $socketID XYZ -10,0,$BZ"]
if {$code != 0} {
    DisplayErrorAndClose $socketID $code "GroupMoveRelative"
return
}

set code [catch "GPIOAnalogSet $socketID GPIO2.DAC1 0"]
if {$code != 0} {
    DisplayErrorAndClose $socketID $code "GPIOAnalogSet"
return
}

puts stdout "Electrodischarge stops"

#####
# Sart fabrication of the second fluid channel

```



```

        set code [catch "PositionerSGammaParametersSet $socketID XYZ.Z 2 400 0.001 0.001"]
            if {$code != 0} {
                DisplayErrorAndClose $socketID $code
            }
    "PositionerSGammaParametersSet"
    return
}

        set code [catch "GroupMoveRelative $socketID XYZ.Z -2"]
            if {$code != 0} {
                DisplayErrorAndClose $socketID $code "GroupMoveRelative"
            }
    return
}

        set code [catch "PositionerSGammaParametersSet $socketID XYZ.X 2 400 0.001 0.001"]
            if {$code != 0} {
                DisplayErrorAndClose $socketID $code
            }
    "PositionerSGammaParametersSet"
    return
}

        set code [catch "PositionerSGammaParametersSet $socketID XYZ.Y 2 400 0.001 0.001"]
            if {$code != 0} {
                DisplayErrorAndClose $socketID $code
            }
    "PositionerSGammaParametersSet"
    return
}

        set code [catch "GroupMoveRelative $socketID XYZ 13.5,3.5,0"]
            if {$code != 0} {
                DisplayErrorAndClose $socketID $code "GroupMoveRelative"
            }
    return
}

FindZero $socketID Z

puts stdout ">>>> Z0 = $Z"

    set Z0 $Z

    set CZ [expr {$Z2 - $Z0}]

# Go up 5 microns plus 0.07

puts stdout "Move Z axis up to start..."

0.001"]
set code [catch "PositionerSGammaParametersSet $socketID XYZ.Z 0.1 400 0.001
if {$code != 0} {
    DisplayErrorAndClose $socketID $code "PositionerSGammaParametersSet"
}
return
}

set code [catch "GroupMoveRelative $socketID XYZ.Z -0.04"]
if {$code != 0} {

```

```

        DisplayErrorAndClose $socketID $code "GroupMoveRelative"
    return
}

# Turn on the power

    set code [catch "GPIOAnalogSet $socketID GPIO2.DAC1 $v"]
    if {$code != 0} {
        DisplayErrorAndClose $socketID $code "GPIOAnalogSet"
    return
    }

    set code [catch "PositionerSGammaParametersSet $socketID XYZ.Z $s 400 0.001
0.001"]
        if {$code != 0} {
            DisplayErrorAndClose $socketID $code
            "PositionerSGammaParametersSet"
            return
        }

        set code [catch "PositionerSGammaParametersSet $socketID XYZ.X $s 400
0.001 0.001"]
            if {$code != 0} {
                DisplayErrorAndClose $socketID $code
                "PositionerSGammaParametersSet"
                return
            }

            set code [catch "PositionerSGammaParametersSet $socketID XYZ.Y $s 400 0.001
0.001"]
                if {$code != 0} {
                    DisplayErrorAndClose $socketID $code
                    "PositionerSGammaParametersSet"
                    return
                }

                puts stdout "Electrodischarge starts for 2D machining..."

                set code [catch "GroupMoveRelative $socketID XYZ -3.5,-3.5,$CZ"]
                if {$code != 0} {
                    DisplayErrorAndClose $socketID $code "GroupMoveRelative"
                return
                }

                #set code [catch "GroupMoveRelative $socketID XYZ -10,0,$BZ"]
                #if {$code != 0} {
                #    DisplayErrorAndClose $socketID $code "GroupMoveRelative"
                #return
                #}

                set code [catch "GPIOAnalogSet $socketID GPIO2.DAC1 0"]
                if {$code != 0} {
                    DisplayErrorAndClose $socketID $code "GPIOAnalogSet"
                return
                }
}

```

```

puts stdout "Electrodischarge stops"

#####
#Move up the Z axis

set code [catch "PositionerSGammaParametersSet $socketID XYZ.Z 1 400
0.001 0.001"]
if {$code != 0} {
    DisplayErrorAndClose $socketID $code
"PositionerSGammaParametersSet"
return
}
set code [catch "GroupMoveRelative $socketID XYZ.Z -2"]
if {$code != 0} {
    DisplayErrorAndClose $socketID $code "GroupMoveRelative"
return
}

puts stdout " First inlet drilling starts"

#}
set code [catch "PositionerSGammaParametersSet $socketID XYZ.X 2 400 0.001 0.001"]
if {$code != 0} {
    DisplayErrorAndClose $socketID $code
"PositionerSGammaParametersSet"
return
}
set code [catch "PositionerSGammaParametersSet $socketID XYZ.Y 2 400 0.001 0.001"]
if {$code != 0} {
    DisplayErrorAndClose $socketID $code
"PositionerSGammaParametersSet"
return
}
set code [catch "GroupMoveRelative $socketID XYZ 3.5,-3.5,0"]
if {$code != 0} {
    DisplayErrorAndClose $socketID $code "GroupMoveRelative"
return
}
}

for {set i 1} {$i<7} {incr i} {

puts stdout "#####"

puts stdout "Starting Fabrication of the $i th hole"

FindZero $socketID Z

set code [catch "PositionerSGammaParametersSet $socketID XYZ.Z 1 400
0.001 0.001"]
if {$code != 0} {

```

```

                                DisplayErrorAndClose          $socketID          $code
"PositionerSGammaParametersSet"
    return
}

    set code [catch "GroupMoveRelative $socketID XYZ.Z 0.7"]
    if {$code != 0} {
        DisplayErrorAndClose $socketID $code "GroupMoveRelative"
    }
    return

    puts stdout "TURN ON THE POWER"

    set code [catch "GPIOAnalogSet $socketID GPIO2.DAC1 $m"]
    if {$code != 0} {
        DisplayErrorAndClose $socketID $code "GPIOAnalogSet"
    }
    return

}

    after $t

    puts stdout "TURN OFF THE POWER"

    set code [catch "GPIOAnalogSet $socketID GPIO2.DAC1 0"]
    if {$code != 0} {
        DisplayErrorAndClose $socketID $code "GPIOAnalogSet"
    }
    return

}

    set code [catch "GroupMoveRelative $socketID XYZ.Z -3"]
    if {$code != 0} {
        DisplayErrorAndClose $socketID $code "GroupMoveRelative"
    }
    return

}

}

#Second hole

    set code [catch "PositionerSGammaParametersSet $socketID XYZ.Z 1 400 0.001 0.001"]
    if {$code != 0} {
        DisplayErrorAndClose          $socketID          $code
"PositionerSGammaParametersSet"
        return
    }

    set code [catch "GroupMoveRelative $socketID XYZ.Z -1"]
    if {$code != 0} {
        DisplayErrorAndClose $socketID $code "GroupMoveRelative"
    }
    return

}

    puts stdout " First inlet drilling starts"

#}

    set code [catch "PositionerSGammaParametersSet $socketID XYZ.X 2 400 0.001 0.001"]

```

```

        if {$code != 0} {
            DisplayErrorAndClose $socketID $code
"PositionerSGammaParametersSet"
        return
    }

    set code [catch "PositionerSGammaParametersSet $socketID XYZ.Y 2 400 0.001 0.001"]
    if {$code != 0} {
        DisplayErrorAndClose $socketID $code
"PositionerSGammaParametersSet"
        return
    }

    set code [catch "GroupMoveRelative $socketID XYZ 0,7,0"]
    if {$code != 0} {
        DisplayErrorAndClose $socketID $code "GroupMoveRelative"
        return
    }

for {set i 1} {$i<7} {incr i} {

    puts stdout "#####"

    puts stdout "Starting Fabrication of the $i th hole"

        FindZero $socketID Z

    set code [catch "PositionerSGammaParametersSet $socketID XYZ.Z 1 400
0.001 0.001"]
    if {$code != 0} {
        DisplayErrorAndClose $socketID $code
"PositionerSGammaParametersSet"
        return
    }

    set code [catch "GroupMoveRelative $socketID XYZ.Z 0.7"]
    if {$code != 0} {
        DisplayErrorAndClose $socketID $code "GroupMoveRelative"
        return
    }

    puts stdout "TURN ON THE POWER"

    set code [catch "GPIOAnalogSet $socketID GPIO2.DAC1 $m"]
    if {$code != 0} {
        DisplayErrorAndClose $socketID $code "GPIOAnalogSet"
        return
    }

    after $t

    puts stdout "TURN OFF THE POWER"

    set code [catch "GPIOAnalogSet $socketID GPIO2.DAC1 0"]

```

```

        if {$code != 0} {
            DisplayErrorAndClose $socketID $code "GPIOAnalogSet"
        }
        return
    }

    set code [catch "GroupMoveRelative $socketID XYZ.Z -3"]
    if {$code != 0} {
        DisplayErrorAndClose $socketID $code "GroupMoveRelative"
    }
    return
}

# Third hole outlet

    set code [catch "PositionerSGammaParametersSet $socketID XYZ.Z 1 400 0.001 0.001"]
    if {$code != 0} {
        DisplayErrorAndClose $socketID $code
        "PositionerSGammaParametersSet"
    }
    return
}

    set code [catch "GroupMoveRelative $socketID XYZ.Z -1"]
    if {$code != 0} {
        DisplayErrorAndClose $socketID $code "GroupMoveRelative"
    }
    return
}

    puts stdout " First inlet drilling starts"

#}

    set code [catch "PositionerSGammaParametersSet $socketID XYZ.X 2 400 0.001 0.001"]
    if {$code != 0} {
        DisplayErrorAndClose $socketID $code
        "PositionerSGammaParametersSet"
    }
    return
}

    set code [catch "PositionerSGammaParametersSet $socketID XYZ.Y 2 400 0.001 0.001"]
    if {$code != 0} {
        DisplayErrorAndClose $socketID $code
        "PositionerSGammaParametersSet"
    }
    return
}

    set code [catch "GroupMoveRelative $socketID XYZ -13.5,-3.5,0"]
    if {$code != 0} {
        DisplayErrorAndClose $socketID $code "GroupMoveRelative"
    }
    return
}

    for {set i 1} {$i<7} {incr i} {

        puts stdout "#####"

        puts stdout "Starting Fabrication of the $i th hole"
    }

```

```

FindZero $socketID Z

set code [catch "PositionerSGammaParametersSet $socketID XYZ.Z 1 400
0.001 0.001"]
if {$code != 0} {
    DisplayErrorAndClose          $socketID          $code
"PositionerSGammaParametersSet"
return
}

set code [catch "GroupMoveRelative $socketID XYZ.Z 0.7"]
if {$code != 0} {
    DisplayErrorAndClose $socketID $code "GroupMoveRelative"
return
}

puts stdout "TURN ON THE POWER"

set code [catch "GPIOAnalogSet $socketID GPIO2.DAC1 $m"]
if {$code != 0} {
    DisplayErrorAndClose $socketID $code "GPIOAnalogSet"
return
}

after $t

puts stdout "TURN OFF THE POWER"

set code [catch "GPIOAnalogSet $socketID GPIO2.DAC1 0"]
if {$code != 0} {
    DisplayErrorAndClose $socketID $code "GPIOAnalogSet"
return
}

set code [catch "GroupMoveRelative $socketID XYZ.Z -3"]
if {$code != 0} {
    DisplayErrorAndClose $socketID $code "GroupMoveRelative"
return
}

}

set code [catch "PositionerSGammaParametersSet $socketID XYZ.Z 1 400 0.001 0.001"]
if {$code != 0} {
    DisplayErrorAndClose          $socketID          $code
"PositionerSGammaParametersSet"
return
}

set code [catch "GroupMoveRelative $socketID XYZ.Z -10"]
if {$code != 0} {
    DisplayErrorAndClose $socketID $code "GroupMoveRelative"
return
}

}

puts stdout ">>>> micro-machining has been successfully finished"

```

```
#####  
# Close TCP socket  
TCP_CloseSocket $socketID
```